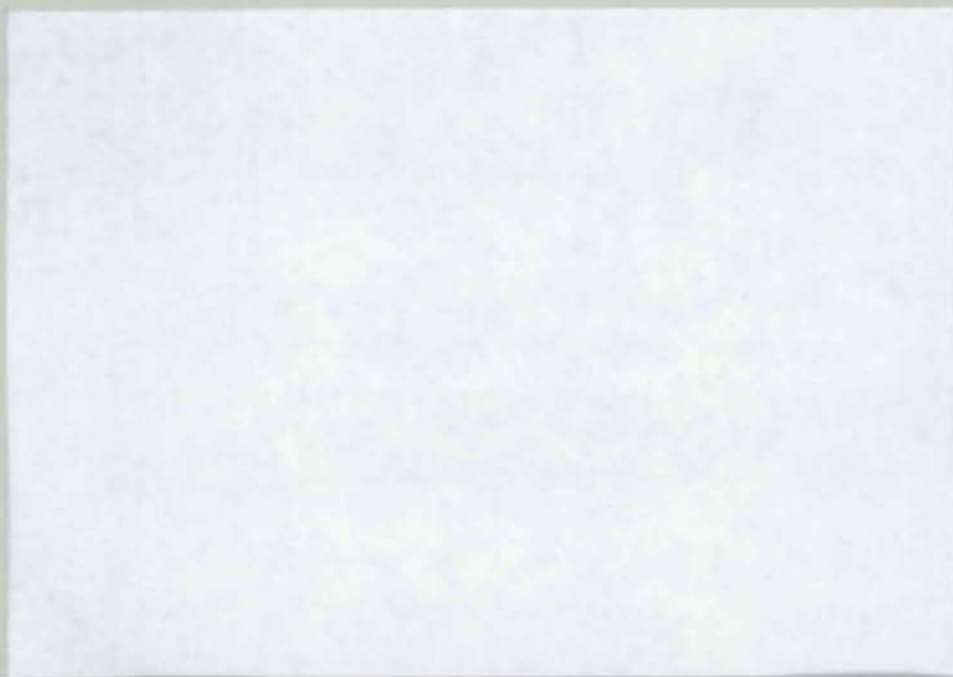Structural Research Studies
Department Of Civil Engineering

Final Report

DEVELOPMENT OF CONNECTION DETAIL FOR CONNECTING STEEL BEAM TO COMPOSITE COLUMNS

key words –
1 – composite
2 – connections

BY

Bangalore A. Pralash
Atorod Azizinamini   main author

Submitted To

American Institute Of Steel Construction

University Of Nebraska-Lincoln
Lincoln, Nebraska
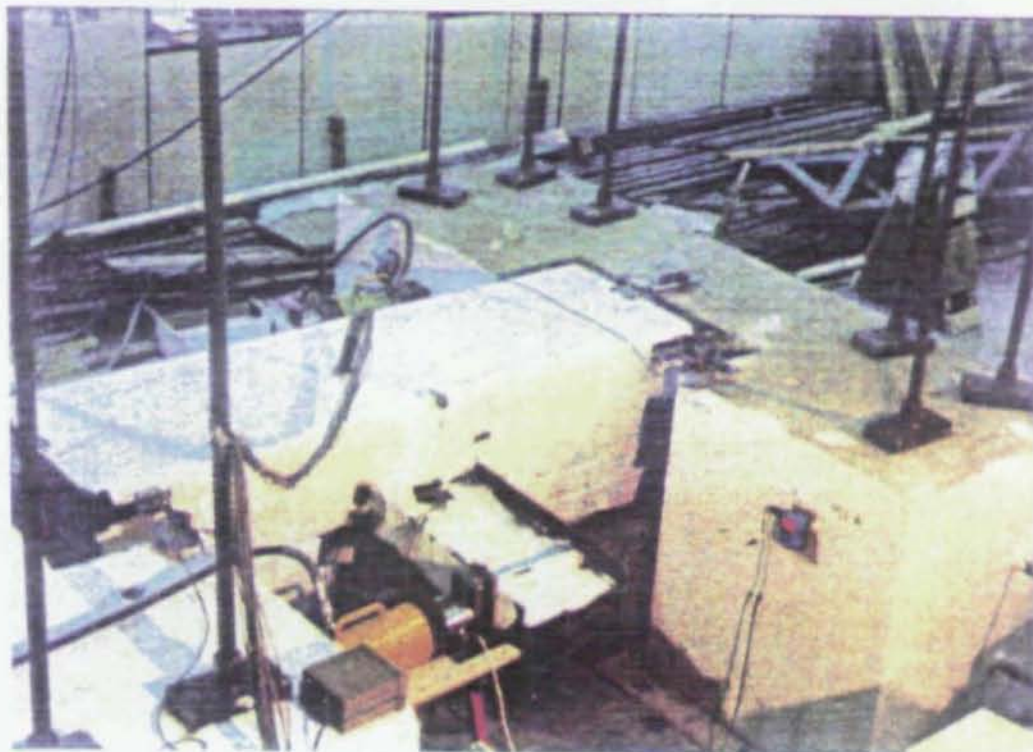December, 1992

PROJECT TEAM

Research Executed By: Department of Civil Engineering
University of Nebraska-Lincoln

Principal Investigator: Dr. Atorod Azizinamini

Graduate Student: Mr. Bangalore A. Prakash

Research Sponsored By: American Institute of Steel Construction
Nebraska Energy Office
Center for Infrastructure Research

ACKNOWLEDGEMENTS

March 1, 1993

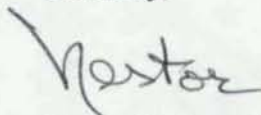To: AISC Committee on Research

Gentlemen:

In preparation for the upcoming Committee meeting during the afternoon of March 16 in Orlando, Florida, enclosed is the Final Report, "Development of Connection Detail for Connecting Steel Beam to Composite Columns," Azizinamini and Pralash, University of Nebraska-Lincoln.

Our appointed Committee on Research membership is the same as in 1992 except for Cliff Ousley replacing Cliff Bengston as Bethlehem Steel Corporation's representative and with the addition of David McKenzie from Havens Steel Company. Welcome!

AISC Design Guide No. 6, "Load and Resistance Factor Design of W-Shapes Encased in Concrete," has recently been released. Enclosed is a complimentary copy. Additional copies may be ordered through AISC Publications.

In addition to the already scheduled research progress reports by Azizinamini and Wallace beginning at 3:00 p.m., Tom Murray has also offered to give a presentation on his seated beam tests relative to web crippling.

Cordially,

Nestor R. Iwankiw
Secretary, AISC Committee on Research

NRI/pab
Enclosures
cc: G. Haaijer
       T. M. Murray

December 23, 1992

Mr. Nestor R. Iwankiw
American Institute of Steel Construction, Inc.
One East Wacker Drive, Suite 3100
Chicago, IL 60601-2001

Dear Nestor:

Enclosed please find two copies of the final report entitled, "Development of Connection Detail for Connecting Steel Beams to Composite Columns." This report was made possible through a $5000 grant we received from AISC. I sincerely appreciate AISC's support and hope we can collaborate on future projects.

I look forward to seeing you at the AISC Conference.

Yours sincerely,

Atorod Azizinamini
Assistant Professor

AA/da

Encl

TABLE OF CONTENTS

LIST OF FIGURES

LIST OF TABLES

CHAPTER 1

INTRODUCTION

1.1 General

Steel and reinforced concrete are frequently combined in composite or mixed structural systems. Mixed structural systems invariably use structural steel for gravity load subsystems and reinforced concrete or composite members for lateral load subsystems. This combination generally results in greater economy and safety than could be achieved by either material alone. A better understanding of the composite behavior is required for an efficient and economical design of composite structural systems.

1.2 Composite Columns

This study is concerned with concrete filled tube columns. In this type of construction the composite column consists of a structural steel shape, pipe, or tube filled with high strength concrete.

Concrete filled tube columns are being used in high-rise structures in the U.S.A and far east Asian countries. Concrete strengths between 8000 to 14000 psi have already been used in this type of construction.

The advantages and disadvantages of a concrete-filled tube column in comparison with a standard reinforced concrete column of same size and same weight of steel are as listed below.

Advantages:

1. Increased ultimate strength

2. Increased stiffness

3. Improved ductility

4. Improved resistance to buckling

5. Elimination of form-work for column construction

Disadvantages:

1. The outside surface of the tube is exposed to the action of fire and it will be necessary to line the column with fire resistant sheeting.

Generally, the overall superior performance of concrete-filled tube column outweighs the additional costs associated with filling the tube and providing fire resistant sheeting.

1.3 Connections to Composite Columns

The economy of mixed systems can be substantially enhanced by designing moment connections between steel beams and the composite columns. Currently there is little

information available for the design of such moment connections. Research is needed for design methods and standardization of moment connections.

The overall objective of this investigation is to develop a feasible and economical connection detail for connecting steel beams to concrete filled tube columns.

CHAPTER 2

REVIEW OF LITERATURE

This chapter presents a review of the available literature on steel beam to composite column connections. Literature available on composite through column connection is limited. To make the review comprehensive, the available literature on other types of relevant composite connections is also presented.

Ansourian[1] studied welded and bolted connections between I-beams and square tubes filled with concrete. Tests were conducted on 9 structural units. The main objectives of this study were: (1) to study continuous frame connections between I-beams of normal and wide flange section and concrete filled tubes, and (2) to study the detailed behavior of rectangular tubes under a range of axial loads varying from 15% to 75% of the collapse load and under the moment loading produced by a beam framing about one of the principal axis.

Tests were done on 3 different sizes of columns: 8 in. x 8 in. x 3/8 in., 10 in. x 10 in. x 1/4 in. and 6 in. x 6 in. x 1/4 in. All the columns were 100 in. long and connected to a 40 in. length of I-beam. These tubes were filled with concrete of compressive strength 5400 psi.

4

Two basic types of connections between the tubes and the normal or wide flanged I-beams were considered. In Type I connections (specimen 1 and 2) as shown in Figure 2.1, the tension component of the beam moment is transferred through a mild steel welded flange plate. The beam shear force is carried by a shear plate. Type II connections were designed such that the tensile force is transferred as a compression on the back of the tube. In specimens 3 and 4, as shown in Figure 2.2, this was done by welding a U-shaped plate to the tension flange and by welding two rectangular bars. A plate was welded to the column to help distribute the concentrated forces. Specimens 5 to 9, as shown in Figure 2.2, were designed as Type II with high strength friction bolts instead of welding.

The failure of the columns was characterized by extensive yielding of the tube walls and outward local buckling. Premature weld failure was observed in Type I connections and hence they are not recommended for use where a high moment transfer is needed. Type II connections developed their full strength. Although this connection develops full strength, the connection detail is complicated with too many connecting elements.

Hawkins, Roeder and Mitchel[14] investigated the connections of steel beams to concrete columns through an embedded steel plate with header studs as shown in Figure 2.3. Tests were conducted on 22 specimens. These tests represent connections in which only a small moment is transferred and the shear transfer dominates. A typical test specimen is shown in Figure 2.4. Shear spans of only 3 to 12 inches were investigated. The loading

simulated balanced gravity load moments. In these connections, moment capacity is severely limited by the tensile capacity of the welds and their vertical spacing. High moments produce high tensile forces in some of the studs and a relatively brittle failure will occur if the tension studs are not deeply embedded. In these tests failure was due to yielding of the stud or pull-out from the concrete.

Mitchel and Kostas[18] have developed an analytical model and design method for precast concrete connections incorporating embedded steel members. The development of this analytical model is based on the results of a series of experiments which included the effects of (1) axial load on column, (2) effective width of connection, (3) presence of reinforcement, (4) shape of embedded member, and (5) eccentricity of loading. The nominal shear capacity of a connection without additional reinforcement is given as:

$$V_c = \frac{0.85 \, f_c' \, b \, l_e}{(1 + 3.6 \, e / l_e)} \tag{2.1}$$

in which e is the eccentricity of V_c measured from the column centroid. The additional nominal shear capacity provided by welded reinforcement is expressed as:

$$V_r = \frac{2 \omega f_c' b l_e}{1 + [6 e l_e / (4.8 s / l_e - 1)]} \tag{2.2}$$

$$\omega = \frac{A_s}{b l_e} \cdot \frac{f_y}{f_c'} \tag{2.3}$$

where s is the distance between symmetrically placed A_s and A_s'. Alternatively, for nonsymmetrically placed reinforcement, s may be taken conservatively as twice the distance from the center of embedment to the nearest welded reinforcement.

Mattock and Gaffar[17] have reported analytical and experimental investigations on the strength of steel sections embedded in reinforced concrete columns as brackets. Based on an assumed stress and strain distribution as shown in Figure 2.5, strength equations were derived for nominal shear and maximum bending moment in embedded section at ultimate load. Experimental studies were done to verify the analytically derived expressions and to examine the effect of width and type of the embedded section on the strength. A typical test specimen used is shown in Figure 2.6. Simplified equations for the design of embedded sections are given as below.

$$V_n = \frac{K_1 \sqrt{t/b} \sqrt{f_c'} b l_e}{0.88 + a / l_e} \tag{2.4}$$

$$M_{max} = V_n (a + l_e/7) \tag{2.5}$$

where, t is the width of the column and a is the eccentricity of V_n, measured from the face of the column. The factor k_1 is taken as 21 if the concrete strength is expressed in psi and t/b < 15.

The Prestressed Concrete Institute[19] committee on connection details, has developed equations for calculating the strength of embedded shapes. The design relationships approximates, conservatively, the bearing conditions occurring at ultimate. Figure 2.7, illustrates the basic approximations used in developing the design equations. The design strength of the section, V_c, is given by:

$$V_c = \frac{0.85 \, f_c' \, b \, l_e}{3 + 3.6 \, e / l_e} \tag{2.6}$$

where f'_c = concrete compressive strength, psi.

 b = effective width of the compression block, in.

 l_e = embedment length, in.

 a = shear span, in.

 e = $a + l_e / 2$, in.

 V_c = nominal strength of the section controlled by concrete, lbs.

The additional capacity of the connection due to reinforcement welded to the embedded is given by:

$$V_r = \frac{2 A_s f_y}{[\dfrac{1 + 6 e / l_e}{4.8 s / l_e - 1}]} \qquad (2.7)$$

where A_s = area of reinforcement, sq.in.

f_y = specified yield strength of the welded rebars, psi

l_e = embedment length, in.

$e = a + l_e / 2$, in.

Chaiki Matsui et.al.[7] have reported tests on composite beam to column connections which makes use of the bond between embossed steel H-shapes and concrete. The embossment was obtained by butt-welding 1/2 in. wide embossed T-shapes to a flat web plate as shown in Figure 2.8. Test results shows that the flange stress will be effectively transferred to the reinforced concrete by means of the embossment.

Hiroshi Kanatani et.al.[15] have performed an experimental study on the concrete filled rectangular hollow section column to H-beam connections fabricated with high strength bolts. Figure 2.9, illustrates the schematic features of the connection used. To prevent the out of plane deformation of the column walls, the steel tubes were partially filled with concrete near the connection in the fabrication shop. Long, high tension bolts were used for easy fabrication without welding in site. The HT bolts were pierced through the concrete filled column and tightened over the split tees or the end plate welded to the beams. The bolts and the encased concrete were unbonded.

In case of specimens with the split tees, slip of shear bolts and the separation between column wall and tee flange has been reported at about 70-80% of the maximum load. At this stage the maximum moments of the beam ends were beyond the plastic moment. The split tee type specimens reached their maximum load, failed by buckling of column flange. The end plate type specimens reached its maximum load at local buckling of column flange or when the end plates collapsed. The behavior of both types of connections was similar.

Sheikh[22,23] has done extensive studies on beam-column moment connections for composite frames. Fifteen two-thirds scale joint specimens were tested under monotonic and cyclic loading to assess strength and stiffness of joints with different details. The connection configuration and reinforcement details used for all 15 specimens is shown in Figure 2.10. The joint shear was mobilized in the test specimens by using stiffener plates. The stiffener plate details are shown in Figure 2.11. The test results have shown that Face Bearing Plates (FBP) substantially enhance joint strength by effectively mobilizing the concrete panel. Variations in the thickness of these plates did not affect the joint capacity. But increase in FBP width has increased the joint strength by about 20%. The results also shows that extending the FBP's above and below the beam was most effective and increased the joint strength by 60% and stiffness by 150%. Increases in joint strength were also observed when shear studs were used to mobilize this field. The principle forces acting on the connection panel and all modes of failure were identified. Based on these a design approach is presented, which can be used to

determine the strength of interior connections between steel beams and concrete columns employing face bearing plates. This design procedure uses basic principles from connection design for steel and reinforced concrete structures by separating the three-dimensional interaction between the steel and concrete into simple mechanisms: the steel web panel, the concrete compression strut, and the concrete compression field.

Deierlein[12] extended the work done by Sheikh[22] on composite connections. Tests were conducted on eight 2/3 scale connections between steel beams and reinforced concrete columns. The specimens were tested under reverse cyclic loading. Various structural steel details were tested in order to assess their influence on the connection strength and stiffness. Details examined included face bearing plates, web stiffener plate, embedded steel column, welded shear studs, steel doubler plates, and vertical joint reinforcement. Figure 2.12, shows the typical test specimen and specimen descriptions. Some of the major findings from his studies are as below:

1. Joint shear strength was enhanced considerably by mobilization of concrete in the joint region.

2. Addition of face bearing plates (FBP) and web stiffener plates mobilized inner joint panel, with resulting strength increase of 50-70% over the plain steel beam. It was also found out that the strength increase was roughly proportional to the FBP width and the FBP thickness had little effect on the strength. Attachments to the beam flanges, such as the steel column, shear studs and extended face bearing plates mobilize the concrete in the outer panel.

3. Attachments to the beam flanges, such as steel columns, shear studs, or extended face bearing plates mobilize the concrete in the outer panel. The steel column and shear stud attachments provided approximately 60% strength increase over the plain steel beam.

4. Joint behavior and connection strength are described in terms of three mechanisms: the steel web and concrete strut mechanisms which carry shear forces in the inner panel region and the concrete compression field mechanism which carries shear in the outer panel region. Analytical design model for calculating the connection capacity using these mechanisms are recommended.

Shakir-Khalil[20] has conducted tests on eight full scale composite connections. The composite columns were comprised of concrete-filled steel circular hollow sections of size 6.63 x 0.2 inch (168.3 x 5 mm). The column tubes were 70.9 inch (1.8 meter) long. End plates of 0.6 inch (15 mm) thickness were welded to the column ends. The beam-column connection was made by using 3.94 x 0.39 inch (100 x 10 mm) fin plates which are fillet welded to the column section. These fin plates were provided with holes for connecting the beam with bolts. Figure 2.13, shows the cross-section of circular hollow tube section with fin plates. Both the column and the beams were loaded. The beam loads were applied at two different eccentricities from the column face: 4.72 inch (120 mm) and 9.45 inch (250 mm). The beam and column load ratio was kept either 1:8 or 1:5. Four of the specimens were provided with 12 shear connectors within the connection length.

Local yielding of the steel tube was observed in the surfaces parallel to the loading plane. Failure was due to the collapse of the upper part of the column section with very little distortion of the steel tube wall at the fin plate level. The test results have shown that the failure load of the connection assembly increases with (1) presence of shear connectors, (2) use of deeper fin plate, and (3) decreasing the lever arm of the beam load.

Shousuke Morino et.al.[24] have investigated three dimensional sub-assemblages of a concrete filled steel tubular column and four H-shaped beams. The specimens were tested under a constant axial load on column, constant beam loads in the minor direction and alternately repeated beam shear in the major direction simulating earthquake loading. Figure 2.14, shows the schematic view of the test setup. The concrete filled tube is 4.92 x 4.92 x 0.24 inch (125 x 125 x 6 mm) in cross-section and the H-shaped built-up steel beams are of size H-250 x 250 x 6 x 9. The specimens were designed for two types of failure modes; shear failure of the connection panel, and flexural failure of the column. In specimens designed for shear failure, the beam-column connection was made by a steel tube of size 4.92 x 4.92 x 0.18 inch (125 x 125 x 4.5 mm) and in specimens designed for flexural failure the connection was made of a box shape built-up section. Diaphragm plates whose thickness was same as that of beam flange pass through the connection and have openings for concrete casting. From the test results, it was found that panel-failing specimens were more stable and exhibit more energy dissipation capacity compared with the column-failing specimens. The panel-failing specimens reached the strength corresponding to the column failure.

14
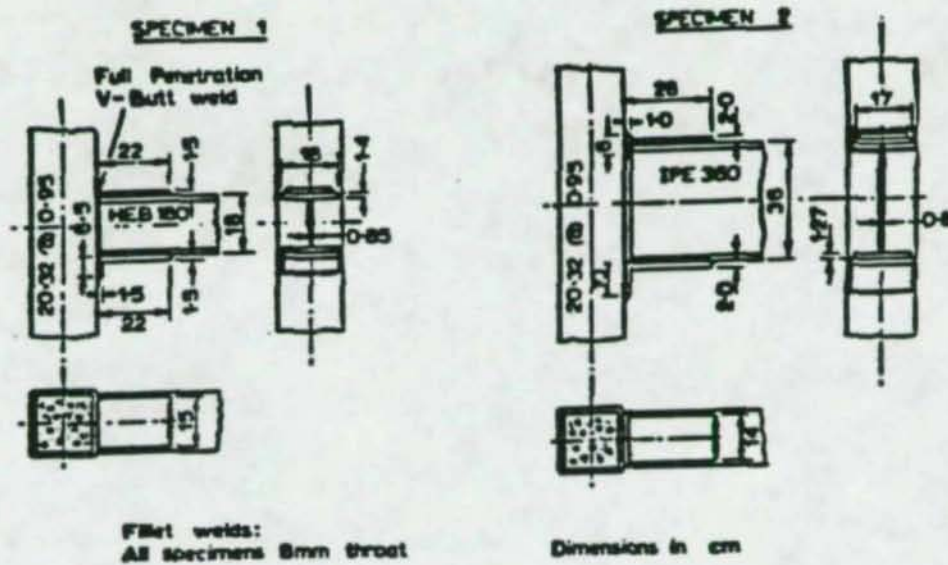
Figure 2.1.   Type I connection detail used by Ansourian[1]

Figure 2.2.   Type II connection detail used by Ansourian[1]
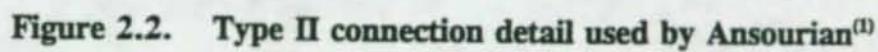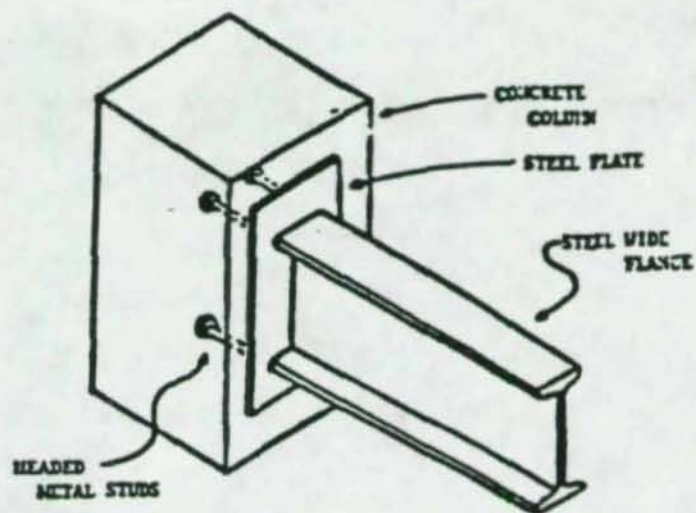
Figure 2.3   Typical steel beam - concrete column connection[16]
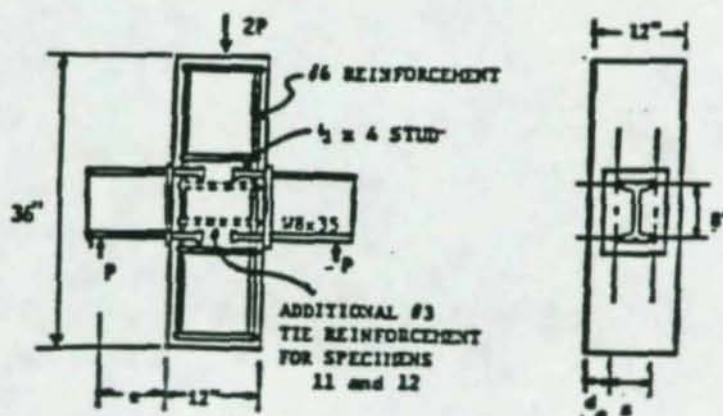
Figure 2.4   Typical test specimen used by Hawkins[14]

17

(a) Actual stresses

(b) Assumed stresses & strains
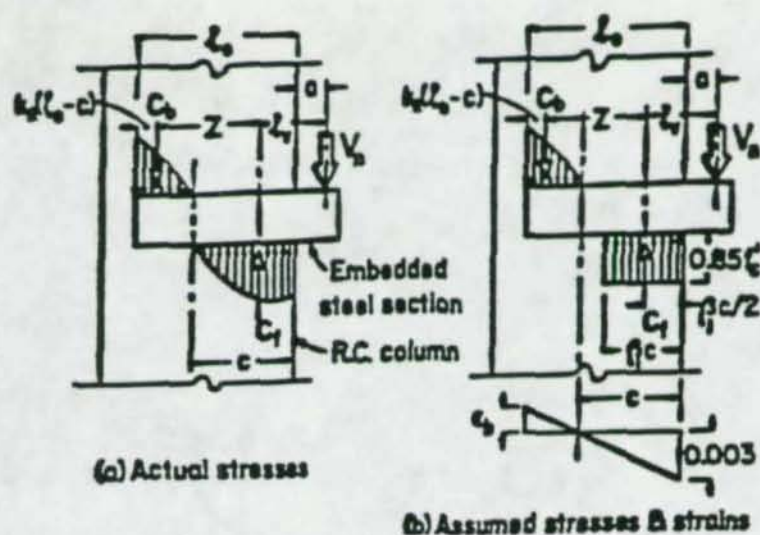
Figure 2.5   Actual and assumed stresses and strains in concrete adjacent to embedded steel section[17]

Figure 2.6   Typical test specimen used by Mattock[17]
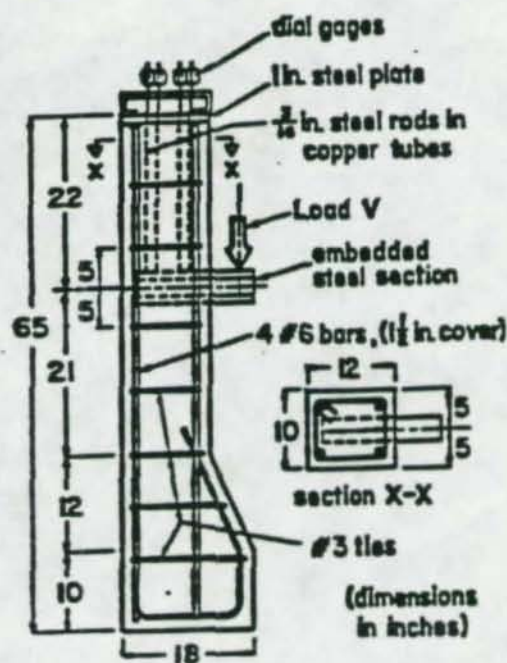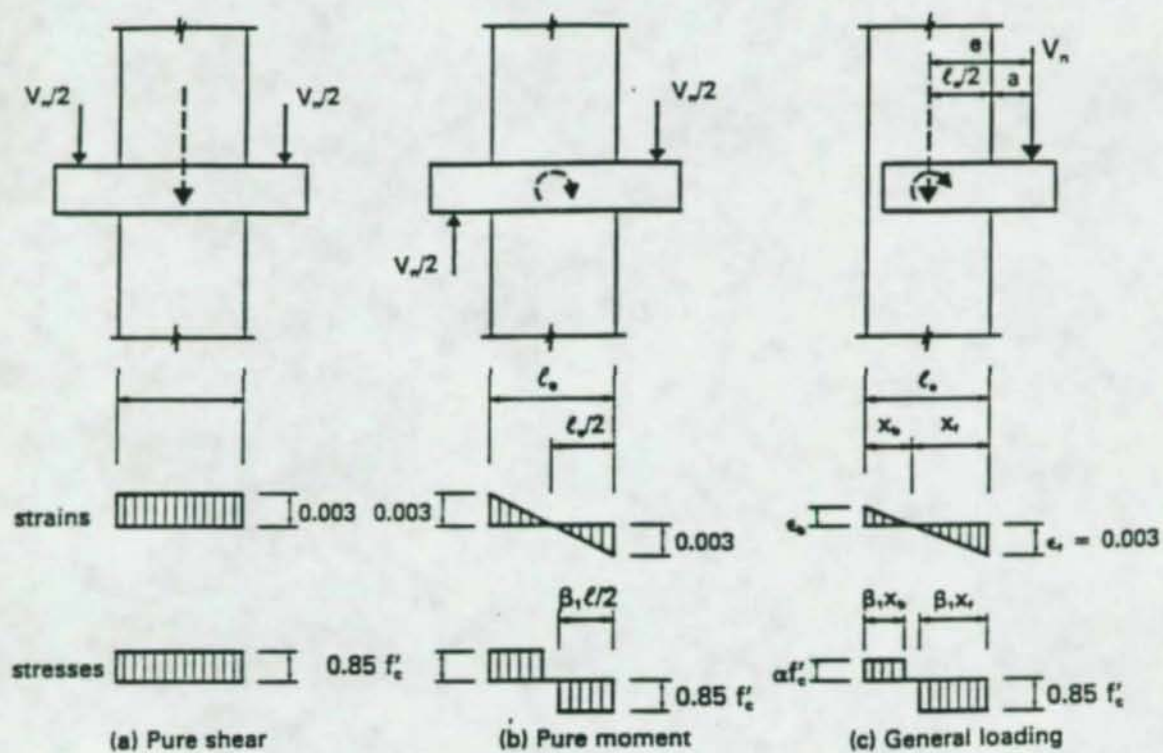
Figure 2.7   Stress-Strain relationship used by PCI[19]
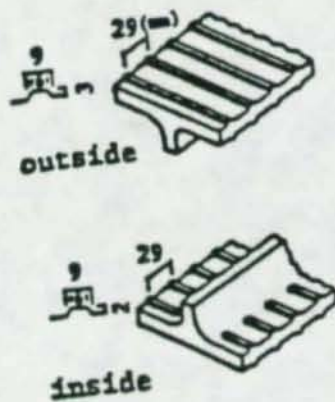
Figure 2.8   Details of embossment used by Chaiki[7]
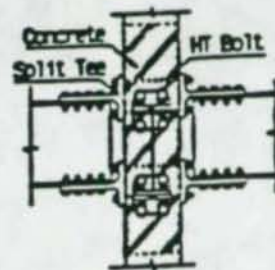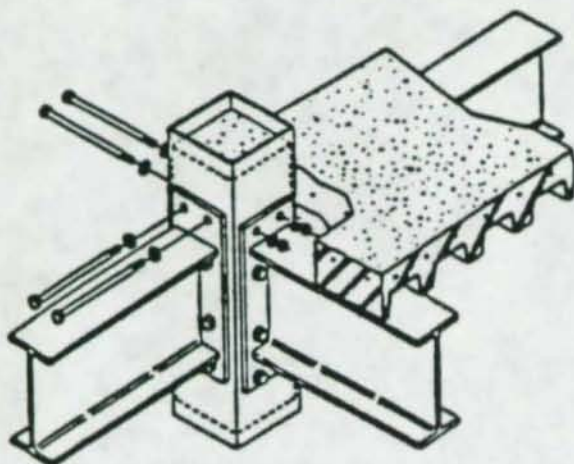
Split tee connection

Figure 2.9   Connection detail used by Hiroshi[15]
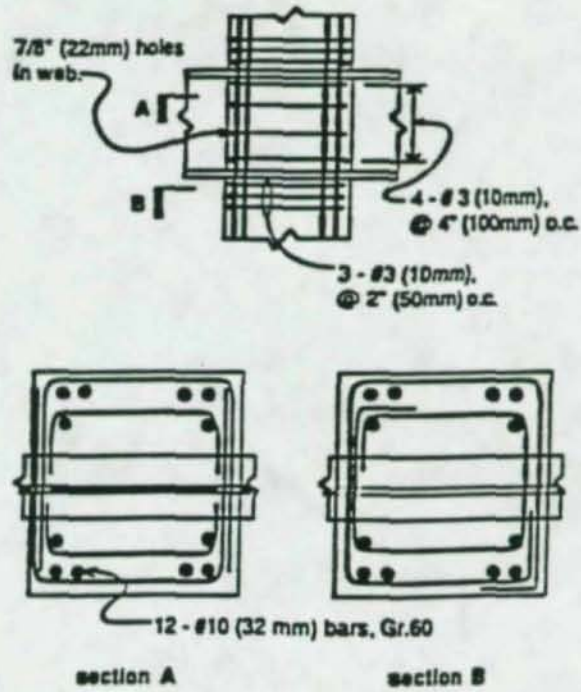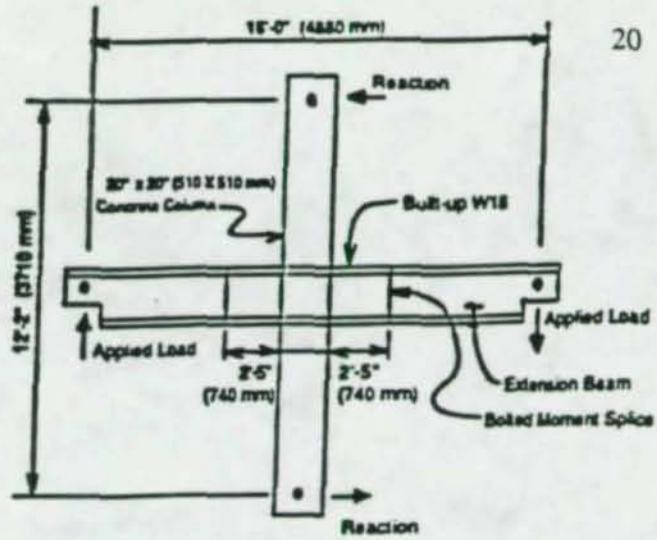
Figure 2.10 Typical test specimen and reinforcing steel detail used by Sheikh[22]
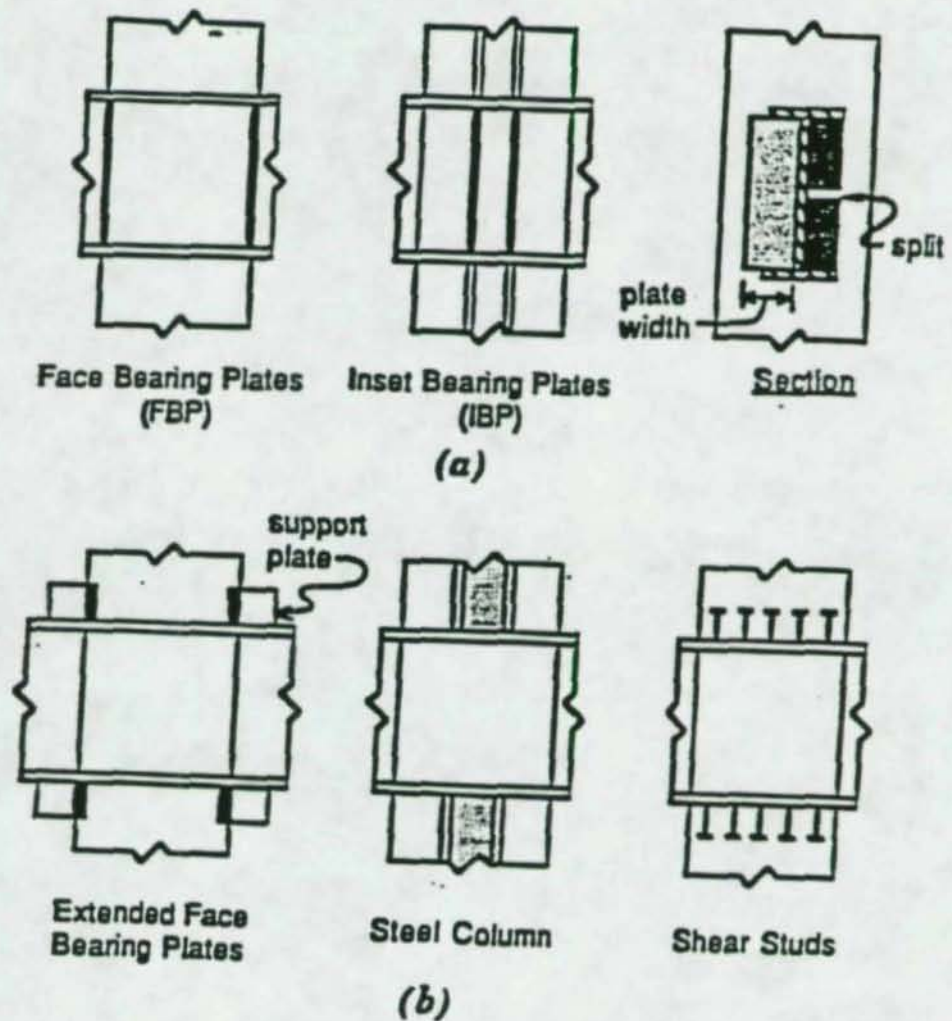
Figure 2.11 (a) Bearing (stiffener) plate detail; (b) Extended FBP, Steel column and Shear stud detail used by Sheikh[22,23]
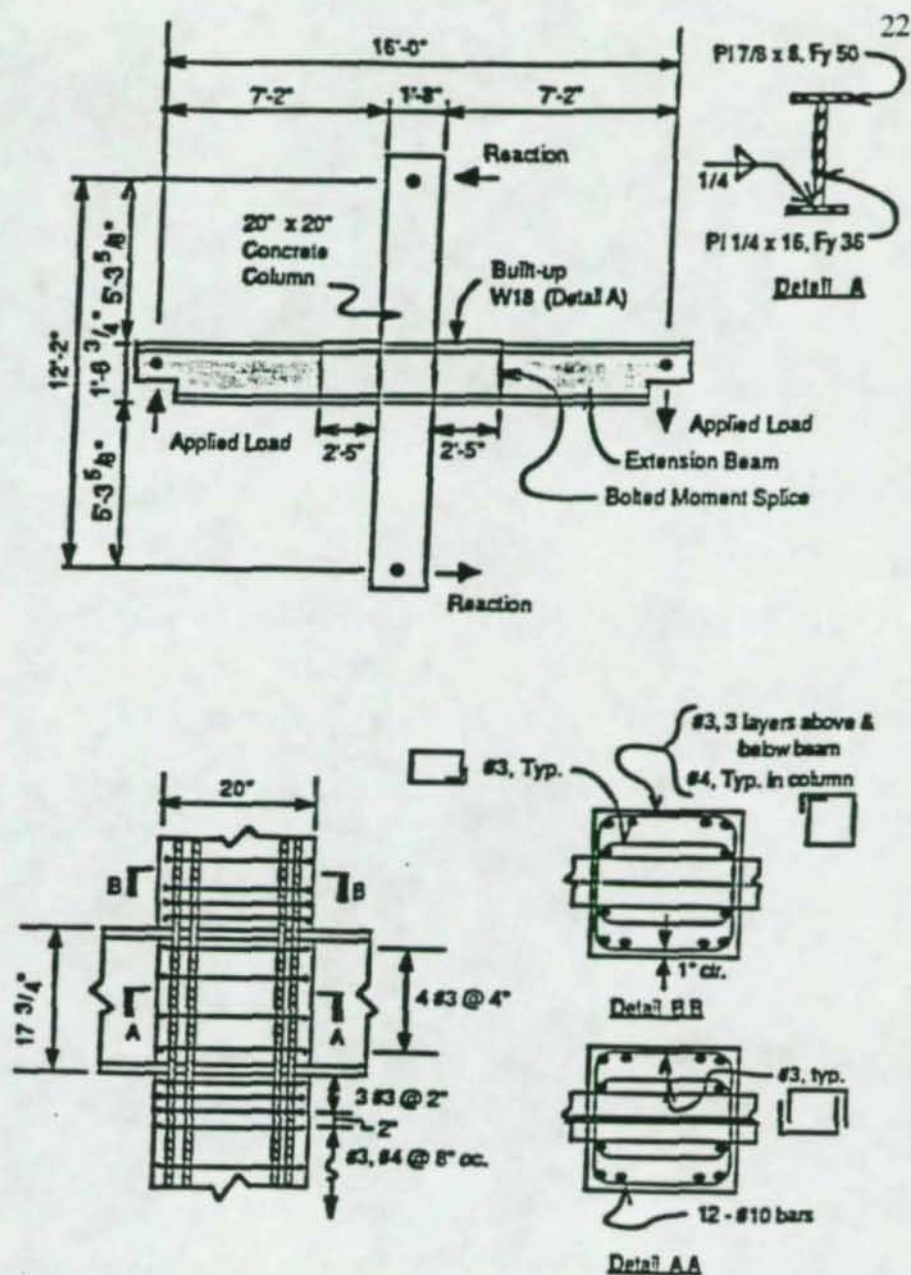
Figure 2.12 Typical test specimen and reinforcing steel details used by Dierlein[12]

1. Cross head   2. Ties
3. Jack + Load cell   4. Base
5. Concrete-filled tube   6. Beams

1. Finplate   2. Beam web
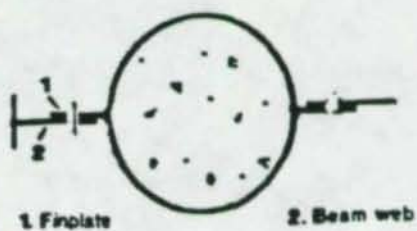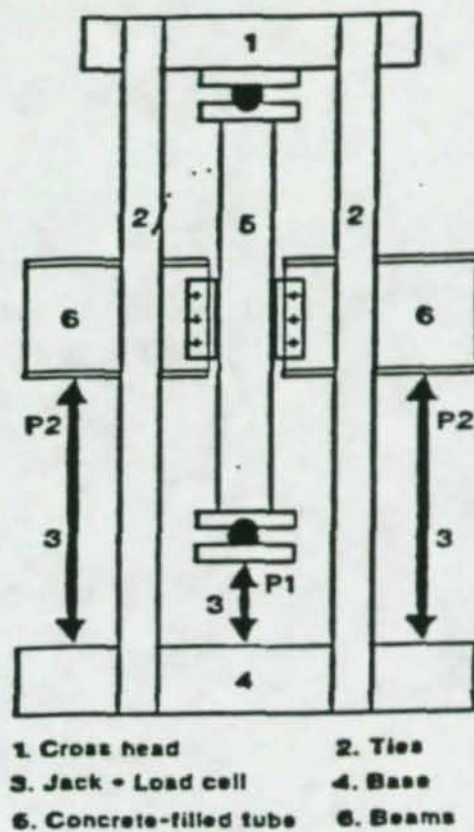
Figure 2.13   Beam-Column connection used by Shakir-Khalil[20]
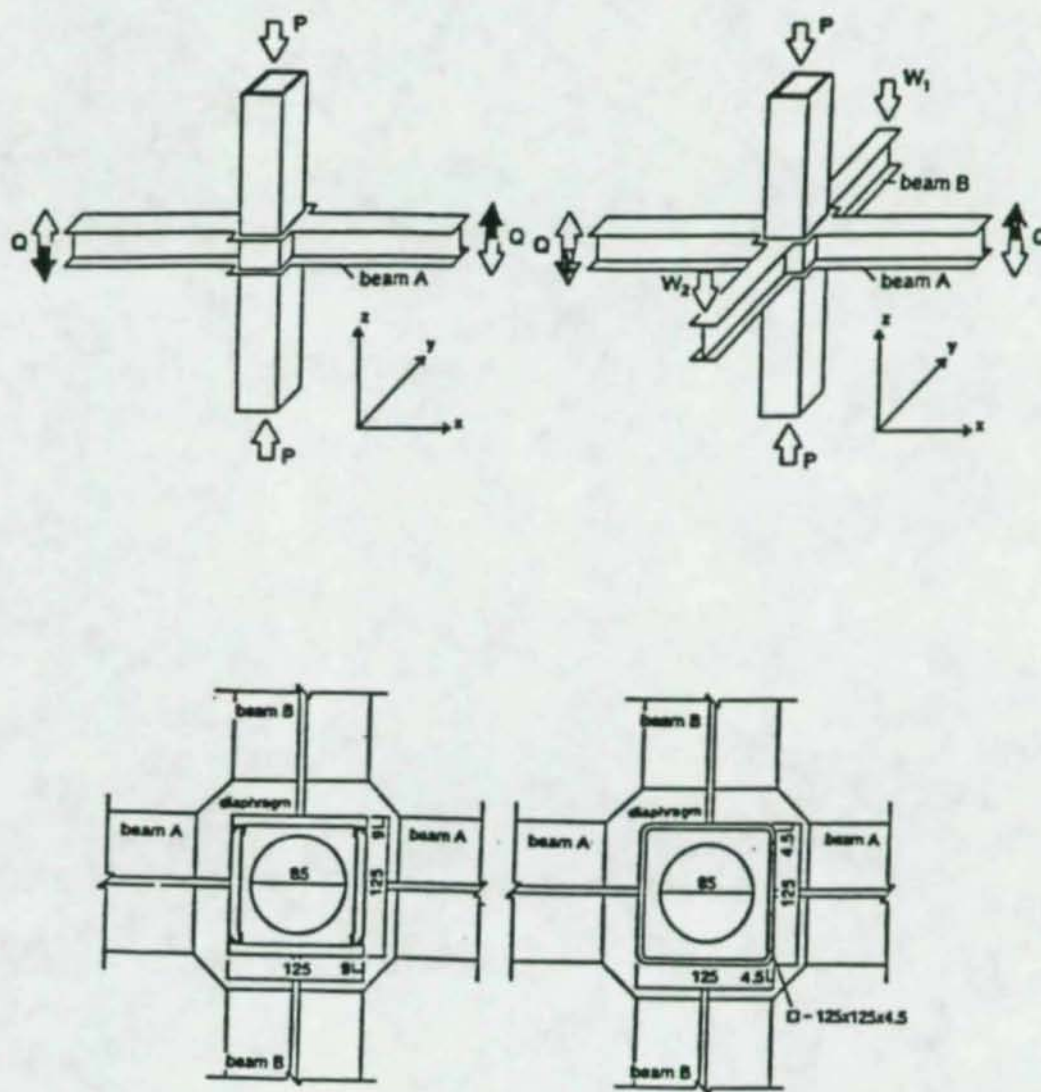
Figure 2.14   Test setup used by Shosuke Morino[24]

CHAPTER 3

DESIGN OBJECTIVES AND SCOPE

3.1 Composite Connections - The Current Practice

The primary function of a composite connection is to transfer large moments between the beams and columns. For the type of composite column which is the focus of this investigation (see Chapter 1), connections between steel beams and the columns are currently made either by directly welding the steel beam to the tube or by using simple shear connections. Often moment connection between the steel beam and composite column is required. There is little information available for the design of these moment connections. Current state of practice for design of composite beam-column joints relies heavily on the individual designers judgement. There is an immediate need for research to develop design guidelines for these connections to ensure safety and improve economy.

3.2 Design Criteria and Options

Proper connection design should ensure satisfactory response of the structure under both service and ultimate conditions. At service loads the joint should have adequate stiffness so as to limit wind and earthquake induced drifts to acceptable limits. The connection

must also exhibit sufficient ductility and resist ultimate design loads at reasonable deformation levels.

Attempts should be made to avoid welding the steel beam or connecting elements directly to the steel tube of the composite column for the following reasons:

(1)   As shown in Figure 3.1, transfer of tensile forces to the steel tube pulls the tube away from the core concrete. This results in over-stressing the steel tube, which is undesirable under cyclic loading. Even if shear studs are used to transfer the tensile forces from steel tube to the core concrete, large stress concentration will develop in the vicinity of the studs. In addition, the deformation of steel tube will increase the connection rotation, thereby decreasing its stiffness.

(2)   Steel tubes are relatively thin compared to other elements of the connection. Under these circumstances welding of connection elements to the tube wall results in large residual stresses.

(3)   The steel tube in a concrete-filled tube column is primarily designed to provide lateral confinement. The additional forces transferred to the tube via the connecting elements will result in over-stressing the steel tube, especially in the case of severe loading conditions.

Considering the above discussion, it is desirable to transfer the forces from the steel beam to the core concrete without over-stressing the steel tube. Three different types of

connections are described below: Connection Type A,B and C. However the recommendation is to use Connection Type C.

3.2.1 Connection Type A:

Figure 3.2 shows connection detail in which forces are transmitted to the core concrete via anchor bolts connecting the steel elements to the steel tube. In this type, all elements are pre-connected to the steel tube in the shop. This type of connection reduces the forces transmitted to the steel tube. The force transferred to concrete is a function of the concrete bond strength. Large magnitude forces cannot be transferred in this way, because the anchor bolts require longer development lengths and it may not be possible to accommodate this development length within the column dimensions. Also, once the bond between concrete and anchor bolts breaks, the force transfer capacity is significantly reduced. Hence this type of connection detail is best suited where a small magnitude of moment transfer is desired.

3.2.2 Connection Type B:

Figure 3.3 shows a second type of connection detail in which the connecting elements are embedded inside the core concrete. Slots are made in the steel tube to accommodate these elements. The effect of the slots on tube stress can be reduced by providing studs in their vicinity.

As shown in figure 3.4, plate A on the top and bottom can be attached to the steel tube during construction using a relatively flexible erection angle. This angle should have relatively large gage length to prevent the transfer of forces to the steel tube due to elongation of plate A. The best approach to support plate B during construction is to use a temporary erection angle.

The ultimate capacity of this detail would be limited to the pull out capacity of the connection elements. For large moment transfer to the core concrete, very stiff connecting elements will be required. Also the connecting elements adequate embedment in to the core concrete.

3.2.3 Connection Type C:

In this third connection type, it is proposed to embed the steel beam inside the concrete-filled tube column. Figure 3.5 shows a steel beam passing through the composite column. Slots are made in the tube wall to pass the beam through. A fillet weld between the beam and the tube wall will hold the connection assembly in position during construction. Inside the tube, a few longitudinal rebars will be welded to the beam flanges. These rebars will help in transferring a portion of the flange forces to the concrete and also restrict the horizontal movement of beam inside the tube under cyclic loading. The beam forces are transferred to the column by a lever arm mechanism as explained in subsequent chapters. This type of connection has a simple detail and is advantageous

from a construction point of view. Complete moment transfer can be achieved in a efficient and economical way.

3.3 Objectives and Scope

The primary objective of this investigation is to develop a reliable connection detail for connecting large size steel beams to steel tubes filled with high strength concrete.

Specifically it was decided to select the Through Beam Connection Detail (Connection Type C described above) as the most promising option and conduct an investigation to comprehend its behavior and suggest design criteria.

Phase I of the research involves detailed three dimensional, nonlinear finite element analysis of the selected composite joint to perform parametric study (Chapter 4).

Phase II of the research involves testing a 1/2 scale model of the selected composite joint assembly in the laboratory (Chapter 5).

A behavioral model and design approach for the selected connection detail are developed from the results of Phases I & II (Chapter 4 & 5).
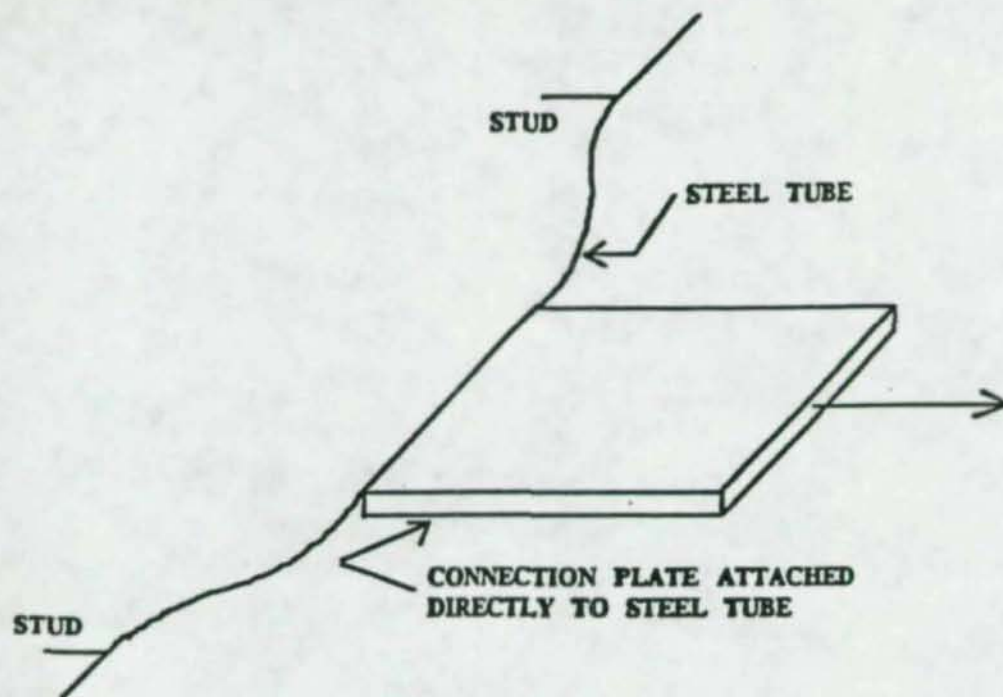
Figure 3.1 Possible bowing effect if the tension force is directly transferred to steel tube
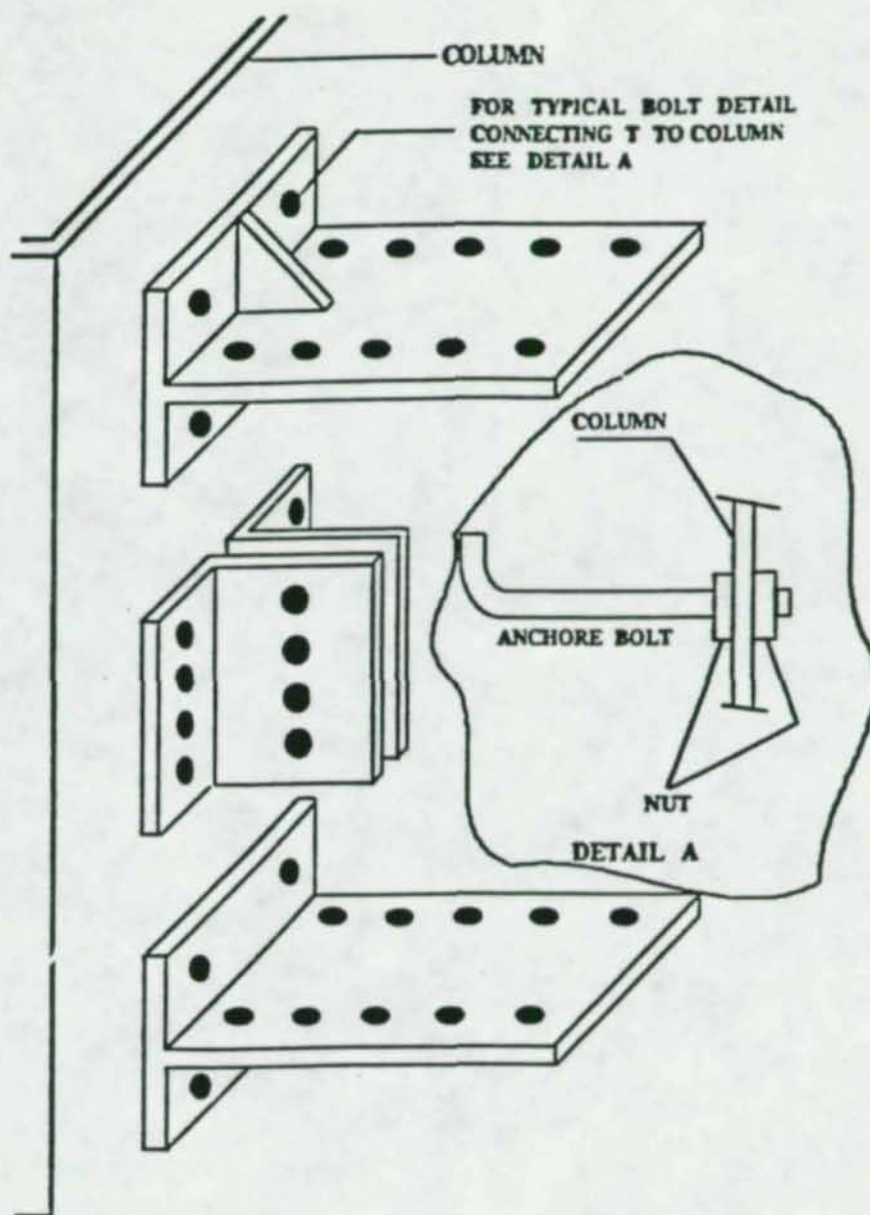
Figure 3.2   Connection Type A

PLATE A

PLATE B

SLOT FOR
PLATE A

SLOT FOR
PLATE B

SLOT FOR
PLATE A
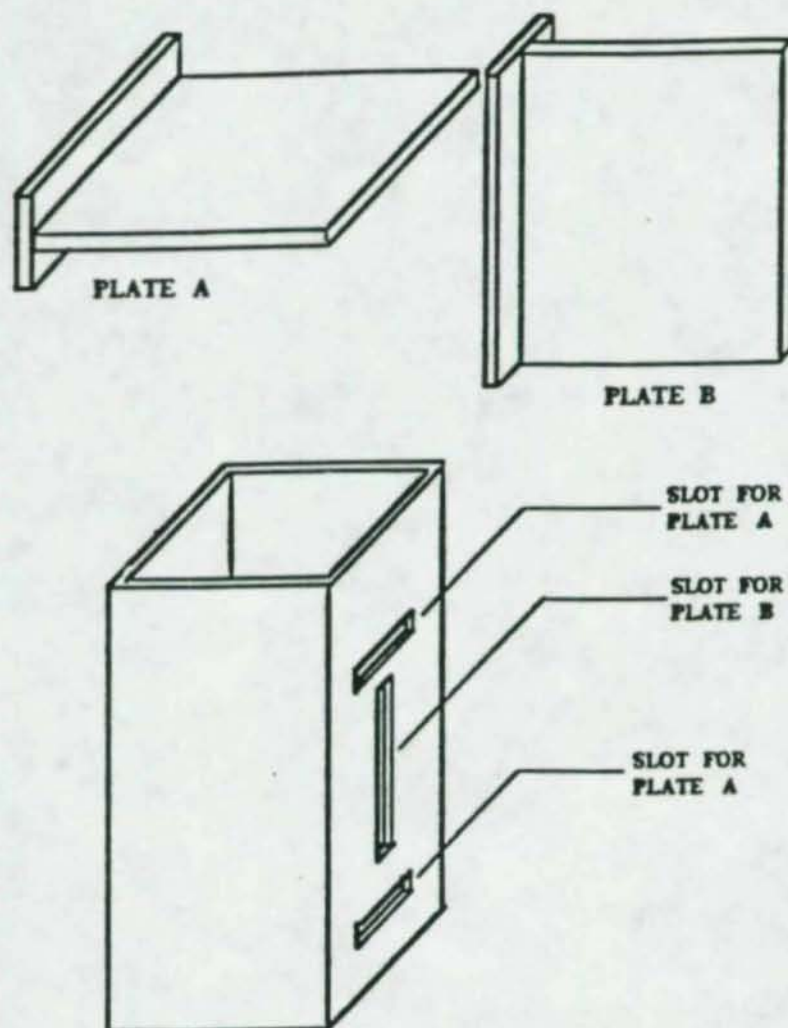
Figure 3.3   Connection Type B

**ERECTION
ANGLE**

**STEEL
TUBE**
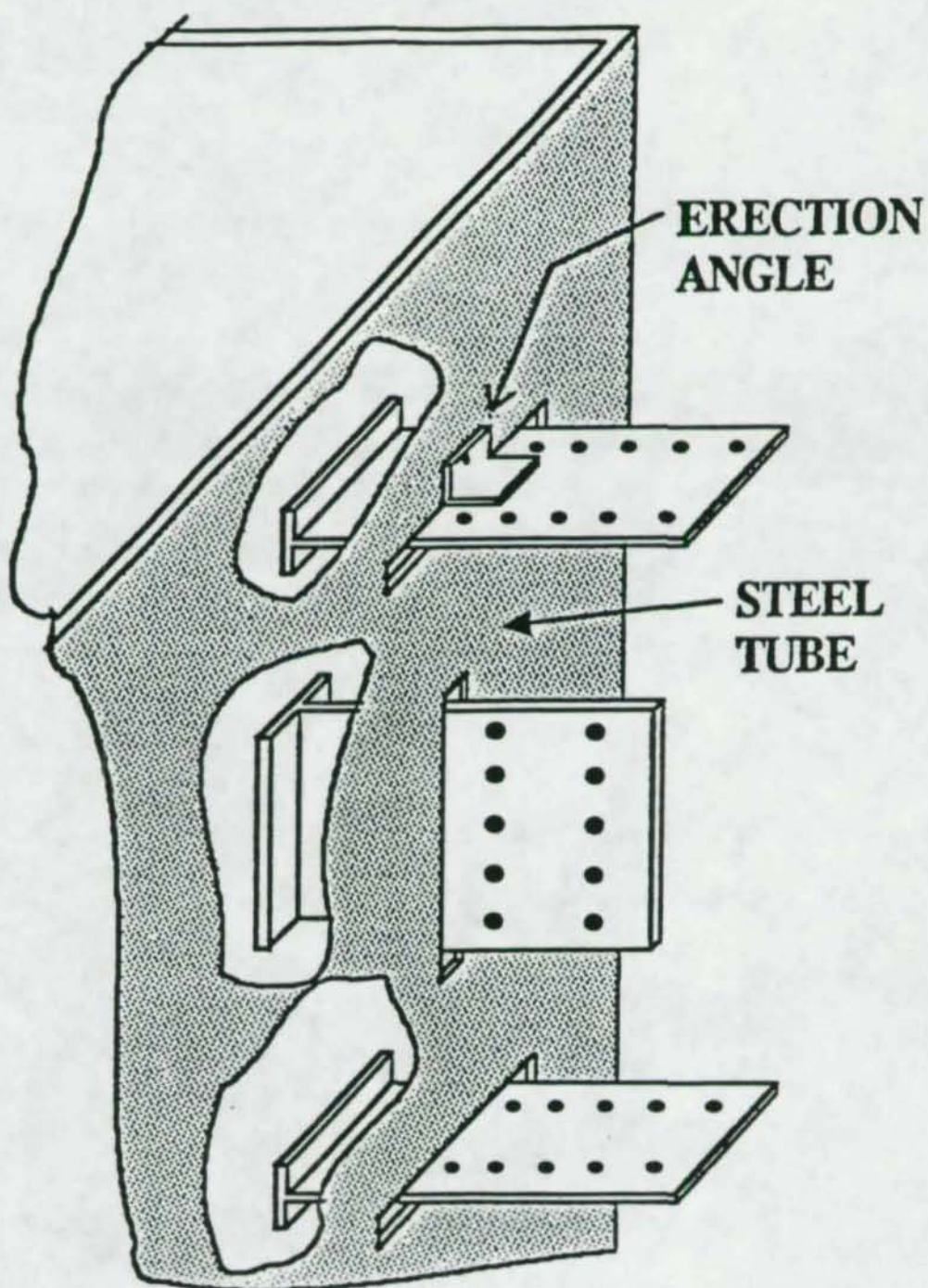
Figure 3.4   Use of Erection Angles for Connection Type B

STEEL TUBE

STEEL
BEAM
PASSING
THROUGH
COLUMN
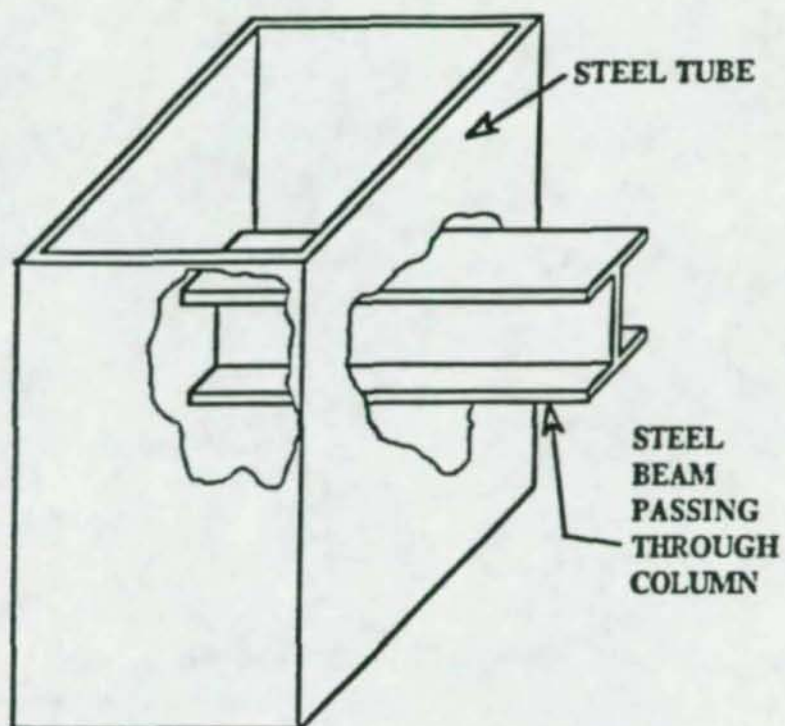
Figure 3.5   Connection Type C

CHAPTER 4

FINITE ELEMENT ANALYSES

4.1 Introduction

This chapter presents the finite element analysis of the through beam connection detail. The type of analysis, parameters studied, and the results are discussed in detail.

The finite element analyses focus on investigating the general behavior of the through beam connection detail configured as interior joints in frames subjected to lateral loading (Figure 4.1). The results of these analyses are used to identify the load transfer mechanism between the steel beam and the composite column in the joint region.

The details of the connection analyzed is shown in Figure 4.2. The detail shown in Figure 4.2 represents an actual detail used in high-rise construction. In this particular building, composite columns consisting of 49 in. x 39 in. (1.25m x 1.0m) rectangular hollow tube sections with 2 in. wall thickness are filled with high strength concrete. These columns, together with heavy steel beams framed in to them at each floor level, form a moment resisting frame. The beams in this particular building are connected directly to the composite columns, with the largest beam size being a W 30x99 section. To prevent over-stressing of the steel tube complicated scheme of stiffener assemblies are

35

provided inside the columns directly against the beam cross section. To thoroughly investigate the effectiveness of this through connection detail, the finite element model uses a 1 in. thick tube rather than a 2 in. thick tube.

Two types of connections are analyzed (Type I and Type II). In the type I connection, the beam is directly connected to the steel tube. In the type II connection, the beam passes completely through the column.

4.2 Finite Element Modelling Details

The ANSYS 4.4A[4] program is used for both modelling and analysis of the composite connection detail. The finite element connection models incorporates the material nonlinearities of both steel and concrete. A detailed 3-D nonlinear model of the entire connection was developed. Making use of symmetry along the beam length, only one-half of the model was generated. Figures 4.3 & 4.4 show the discretization of the two types of connections being analyzed. Figure 4.3 shows the discretization of the direct connection detail. This connection is idealized by providing common nodes for steel tube and steel beam at the joint interface. This model consists of 1244 nodes, 684 concrete elements, 420 shell elements and 180 gap elements. Figure 4.4 shows the discretization of through connection detail. This model is similar to the direct connection model except that the beam passes through the column and gap elements are provided at all nodes

between the steel beam and the surrounding concrete. This model is comprised of 1364 nodes, 684 concrete elements, 498 shell elements, and 300 gap elements.

In these models, the concrete is idealized using 3-D reinforced concrete solid elements (stif 65 of ANSYS). This element is capable of cracking in tension and crushing in compression. The element is defined by eight nodal points having 3 degrees of freedom at each node: translations in nodal x, y and z directions. The most important aspect of this element is its treatment of nonlinear material properties. The concrete is capable of cracking (in 3 orthogonal directions), crushing, plastic deformation and creep. **For all analyses the yield stress of concrete was fictitiously increased so that cracking/crushing occurs before plasticity.** The nonlinear material data used for concrete are as follows:

Modulus of elasticity = 5700 ksi

Yield stress = 1e08 ksi

shear transfer coefficient for open crack = 0.5

shear transfer coefficient for closed crack = 0.1

Uniaxial tensile capacity of concrete = 0.5 ksi

Uniaxial compressive strength of concrete = 10 ksi

Iteration procedure used = Modified Newton-Raphson method.

The steel tube and the steel beam are modelled by using plastic quadrilateral shell elements (stif 43 of ANSYS). This element has 6 degrees of freedom at each node:

translations along nodal x, y and z directions and rotations about nodal x, y and z directions. The displacement functions for this element are linear in both in-plane directions. For the out-of-plane displacement, it uses a mixed interpolation of tensorial components. The element has plasticity, creep, stress stiffening and large deflection capabilities, and is defined by 4 nodal points and 4 thicknesses.

Classical Bi-Linear Kinematic Hardening is used for the steel material. The elastic slope is 29000 ksi and the plastic slope is 900 ksi. The material has a yield stress of 36 ksi.

As shown in Figure 4.5, the interface between steel and concrete is modelled using 3-D interface elements. This element represents two surfaces which may maintain or break physical contact and may slide relative to each other. The element is capable of supporting only compression in the direction normal to the surfaces and shear in the tangential direction. The element is defined by two nodal points with 3 degrees of freedom at each node: translation in the nodal x, y and z directions.

The element may be initially pre-loaded in the normal direction or it may be given a gap specification. In all the analyses a gap specification of zero is used. A high stiffness value of 1e08 kip/in is specified for both normal and tangential directions. Initially the gap was closed and nonsliding. The orientation of the interface is defined by the nodal point location. In analyzing the connection detail with the beam passing completely through the column, gap elements are provided at all points of contact between concrete

and steel beam. Gap elements were provided as shown in Figure 4.6 at selected location, between the steel tube and the surrounding concrete. The points at which the concrete and steel tube have common nodes represent shear stud locations.

Loading is achieved by applying loads to each end of the beams simulating the applied shear and moment at the beam-column junction. The magnitude and direction of the applied shear and moment are equal and opposite to each other. The loading is applied in several small steps and at each step the solution is iterated to convergence.

4.3 Results of Finite Element Analyses

4.3.1 Behavior of Direct Connection Detail:

Very high stresses are observed in both the steel tube and concrete in the joint region. Near the joint interface, the steel tube separates from the concrete resulting in high tensile stresses in the tube wall. The tube wall starts to yield when the load on the beam is about 50% of the yield shear capacity of the beam. The magnitude of compressive stresses in steel tube are about three times lower than the tensile stresses. Figures 4.7 & 4.9, show the stress distribution pattern in the steel tube wall to which the beam was directly connected. Directly behind the beam cross-section, where the beam bears against concrete, the concrete experienced significantly high compressive stresses. At locations where the steel tube and concrete had common nodes (i.e., those points modelling the shear stud locations), high tensile stresses are developed in the concrete.

4.3.2 Behavior of Through Connection Detail:

Figure 4.11, shows the force transfer mechanism observed from the analyses on the through connection detail. The portion of the steel tube between the beam flanges acts as a stiffener, resulting in mobilizing a concrete compression strut which assists the beam web within the joint in carrying shear. The width of the concrete compression strut on each side of the beam web in the direction normal to the beam web is approximately equal to half the beam flange width.

A compressive force block is created when the beam flanges are compressed against the upper and lower columns. The width of this compression block is approximately equal to the width of beam flange. In the Figure 4.11, the compressive force C is shown to be balanced by the tensile force provided by an embedded rod in the concrete and possibly welded to the beam flanges. This rod was not modelled in the finite element analyses, forcing the steel tube to carry this tensile force.

4.4 Comparison of Direct and Through Connection Details

Table 4.1 and Figures 4.7 to 4.10, give a comparison of the two connection details analyzed. The advantages of the through connection detail over the direct connection detail are listed below.

(1) greater than 300% reduction in magnitude of tensile stresses in steel tube, (2) greater than 150% reduction in magnitude of compressive stresses in steel tube, (3) greater than 500% reduction in the magnitude of tube separation from concrete at the joint interface, and (4) greater than 50% reduction in the magnitude of stresses transferred to concrete.

4.5 Conclusions from Finite Element Analysis

The analyses on the direct connection detail reveal that directly connecting the steel beam to the column subjects the steel tube to high stress concentrations resulting in separation of the tube from concrete. This high stress concentration in the tube wall could become a major design problem, especially in the event of cyclic loading, resulting in the formation of fatigue cracks in the steel tube. Also the concrete located behind the beam cross-section will experience severe cracking and crushing thereby reducing the load carrying capacity of both column and connection. Results from the analyses on through connection detail shows that this detail is very effective in overcoming the drawbacks observed in the direct connection detail. As shown in the force transfer mechanism, the compressive force **C** must balance the tensile force **T**. In the finite element model this is achieved forces in the steel tube wall. Welding rebar to the beam flanges near the tube wall can reduce these stresses. The presence of these bars stiffens the beam web within the joint and reduces the stress level in the tube. Also these rods can prevent sliding of beam inside the joint under cyclic loading.

Table 4.1 Comparison of direct and through connections details

Item		Direct Connection	Through Connection
Stresses in steel tube (sig Y) (ksi)	Maximum	39.7	12.4
	Minimum	-13.5	-9.7
Stresses in steel tube (sig Z) (ksi)	Maximum	27.1	7.1
	Minimum	-7.9	-4.3
Maximum tube separation near the joint interface (in.)		0.0686	0.0124
Stresses in concrete enclosed between the beam flanges (ksi)	Maximum	5.4	2.2
	Minimum	-9.6	-4.0
Stresses in concrete outside the beam flanges (ksi)	Maximum	2.1	1.6
	Minimum	-4.6	-1.9

Note: Negative sign for stress magnitude indicates compression
Refer to Figures 4.7 to 4.10 for location and direction of stresses
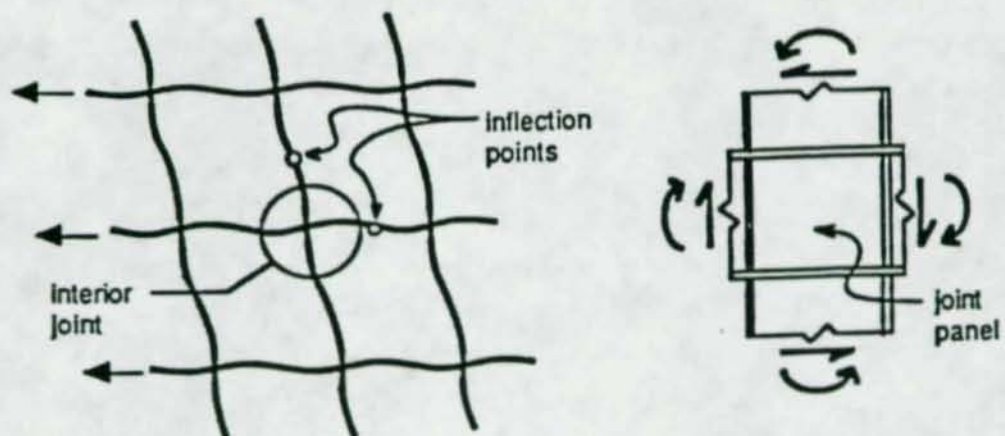
Figure 4.1   Behavior of the frame under lateral loading
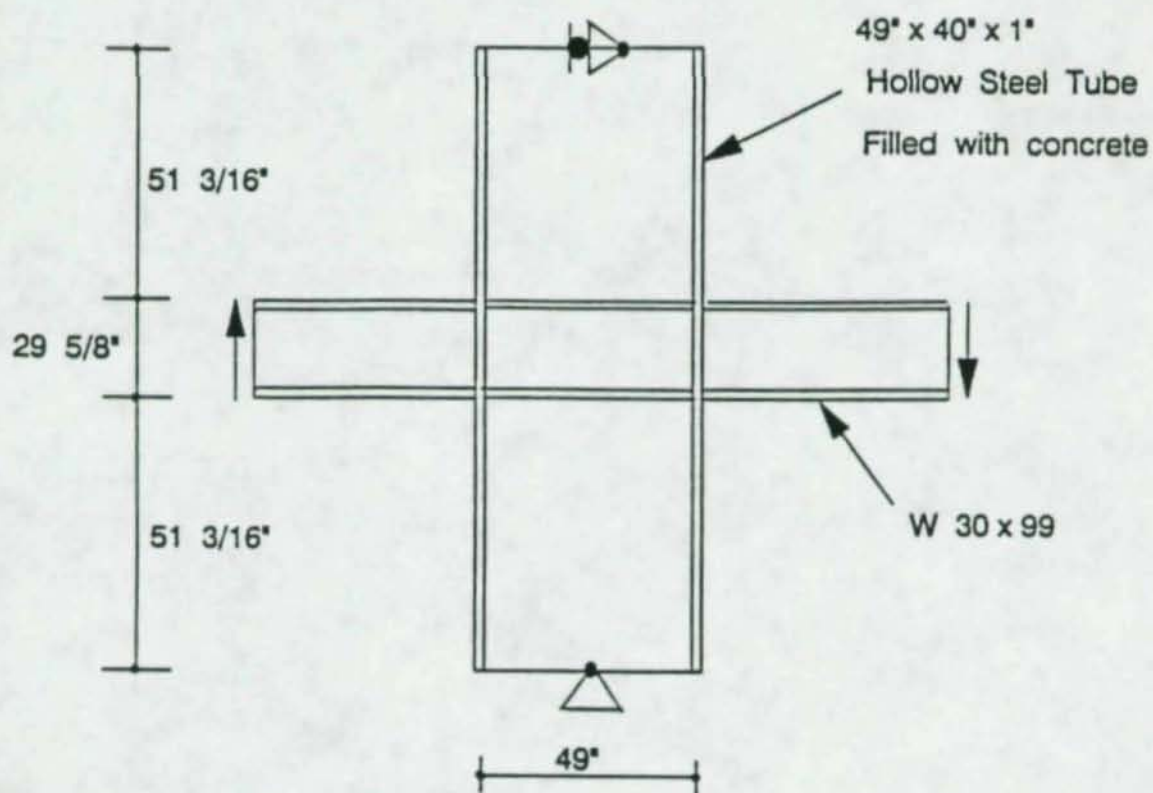
Figure 4.2   Specimen detail used for finite element analyses

FIGURE 4.3   DISCRETIZATION OF DIRECT CONNECTION
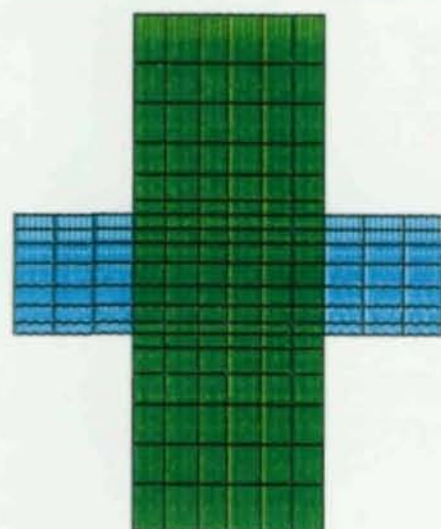
ANSYS 4.4A
AUG 13 1992
21:25:18
POST1 ELEMENTS
TYPE NUM

ZV =1
DIST=71.5
XF =24.605
YF =-65
ZF =-9.84
CENTROID HIDDEN

POST1 ELEMENTS
TYPE NUM
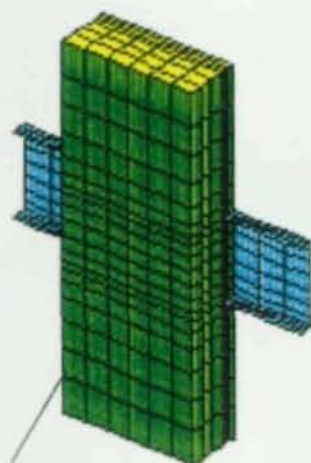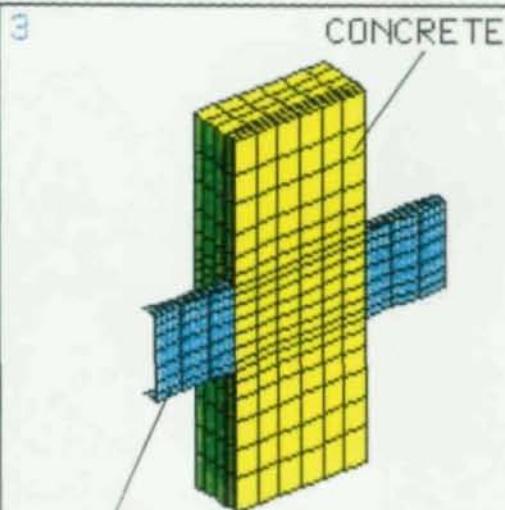
WIND=2
XV =1
YV =1
ZV =1.3
DIST=84.457
XF =24.605
YF =-65
ZF =-9.84
PRECISE HIDDEN

POST1 ELEMENTS
TYPE NUM

WIND=3
XV =1
YV =1
ZV =-1.3

CONCRETE

STEEL TUBE

STEEL BEAM

FIGURE 4.4   DISCRETIZATION OF THROUGH CONNECTION

3-D Reinforced Concrete Element

4 Node Quadrilateral Plastic Shell Element
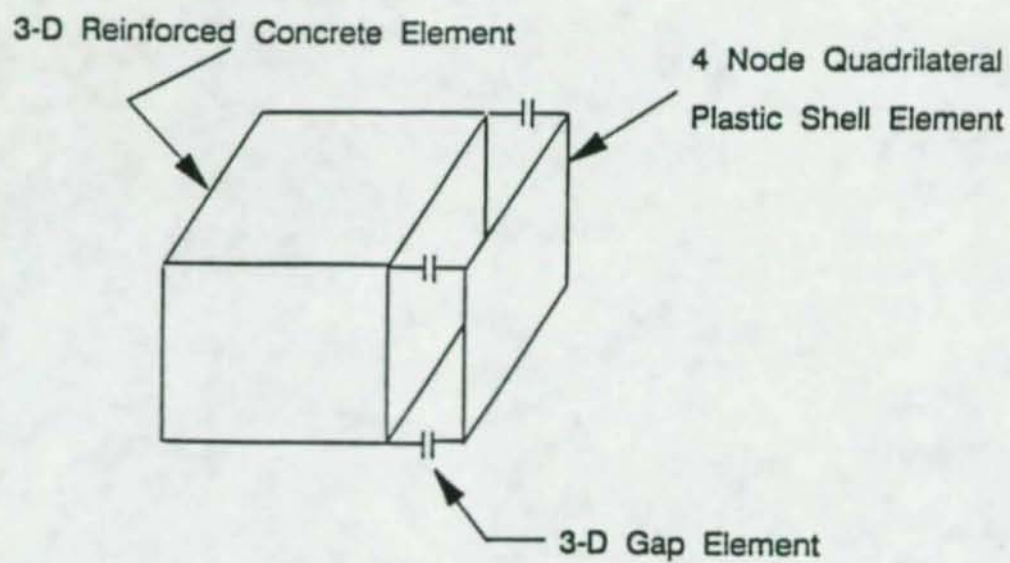
3-D Gap Element

Figure 4.5   Modelling of the steel-concrete interface
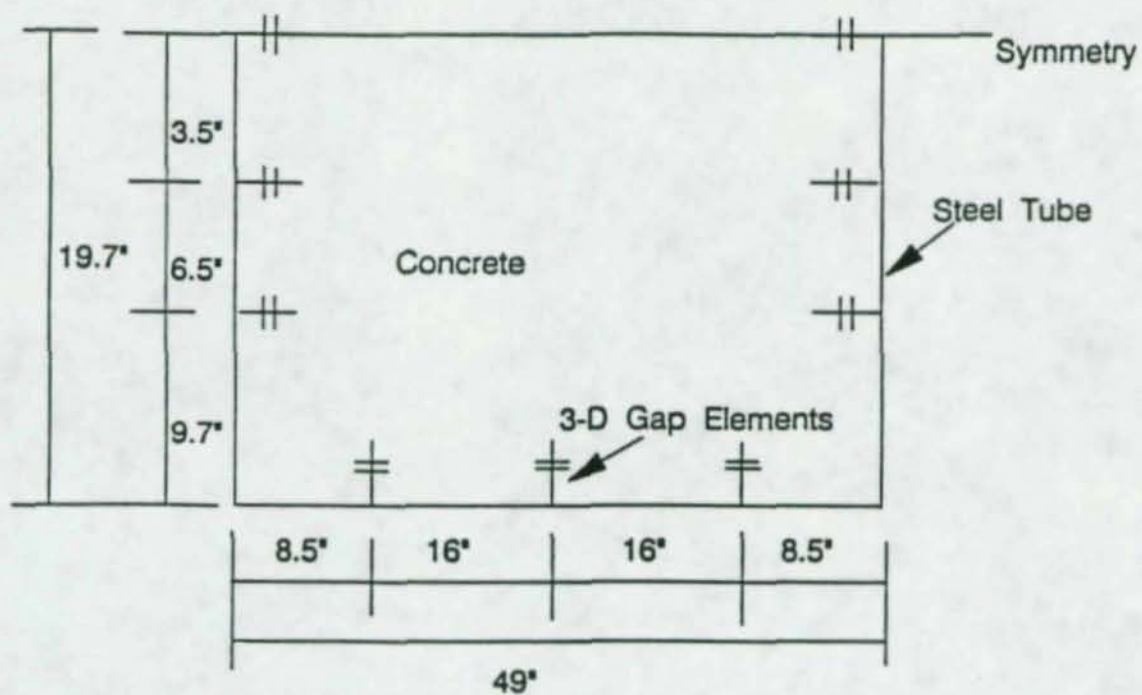
Figure 4.6   Location of gap elements between steel tube and concrete
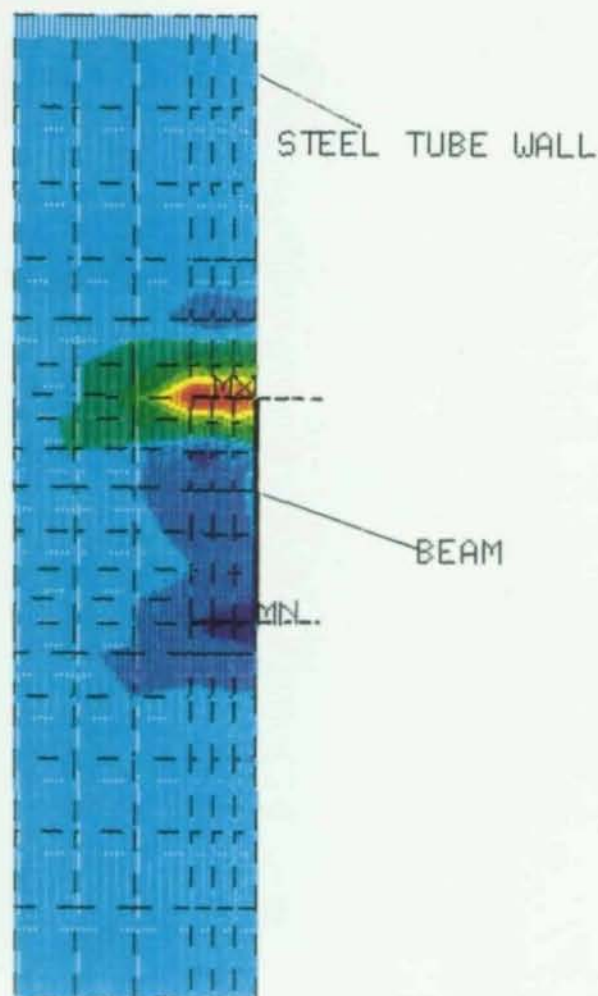
ANSYS 4.4A
AUG 13 1992
20:58:21
POST1 STRESS
STEP=5
ITER=100
SY   (AVG)
TOP
S GLOBAL
DMX =0.06861
SMN =-13.483
SMX =39.737

XV =1
*DIST=71.5
XF =24.605
YF =-65
ZF =-9.839
XRTO=1.63
CENTROID HIDDEN
        -13.483
        -7.57
        -1.656
        4.257
        10.17
        16.084
        21.997
        27.911
        33.824
        39.737

FIGURE 4.7   Vertical stress distribution in steel tube wall to which
          the beam is connected - Direct Connection

ANSYS   4.4A
AUG 13 1992
21:39:33
POST1 STRESS
STEP=1
ITER=100
SY   (AVG)
TOP
S GLOBAL
DMX =0.012397
SMN =-9.734
SMX =12.444

XV =1
DIST=71.5
XF =24.605
YF =-65
ZF =-9.84
XRTO=1.63
CENTROID HIDDEN
-9.734
-7.27
-4.806
-2.341
0.122855
2.587
5.051
7.515
9.98
12.444

STEEL TUBE WALL
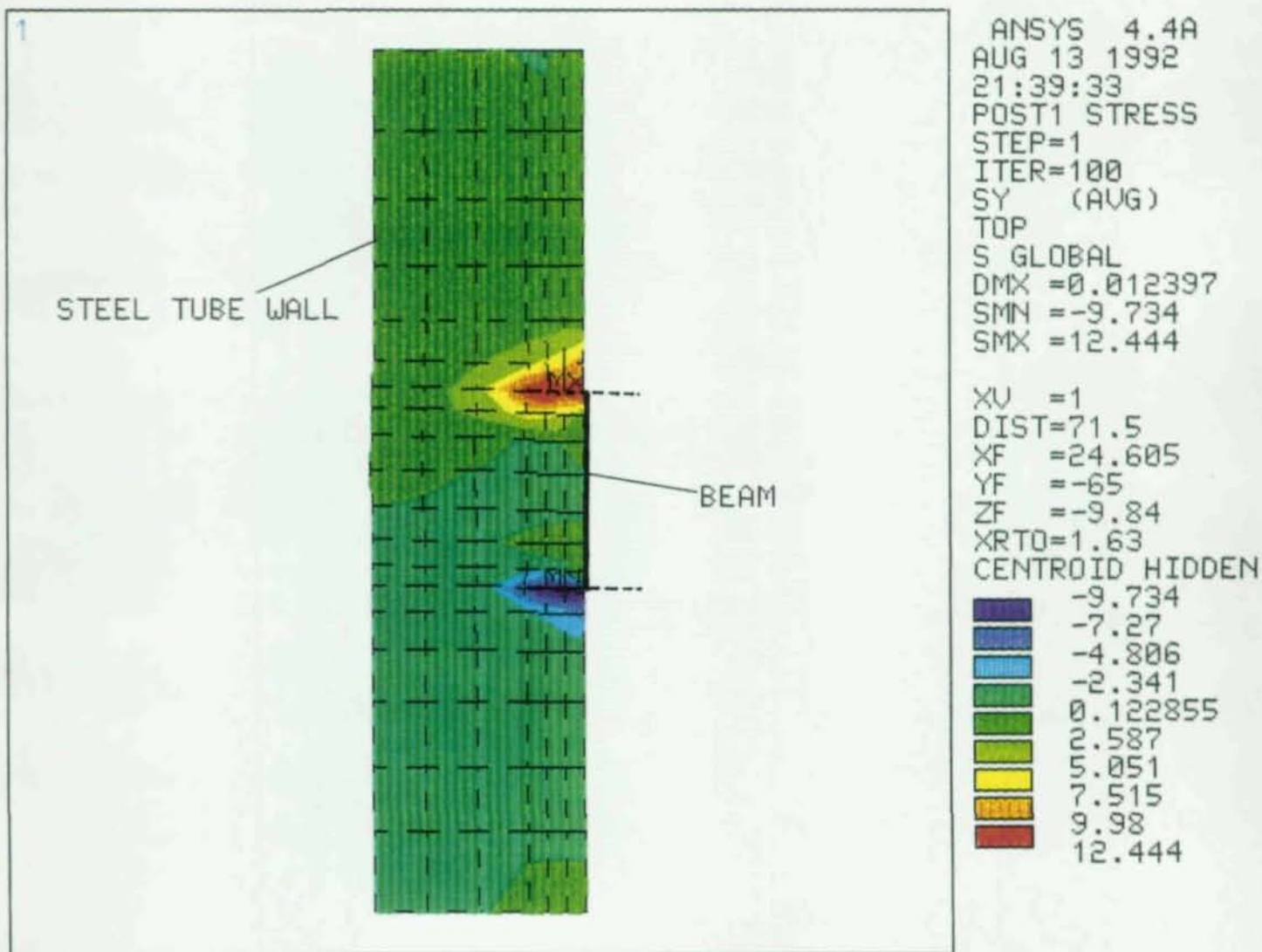
BEAM

Figure 4.8   Vertical stress distribution in steel tube wall
to which beam is connected - Through Connection

Figure 4.9 Horizontal stress distribution in steel tube wall to
which beam is connected - Direct Connection

STEEL TUBE WALL

BEAM
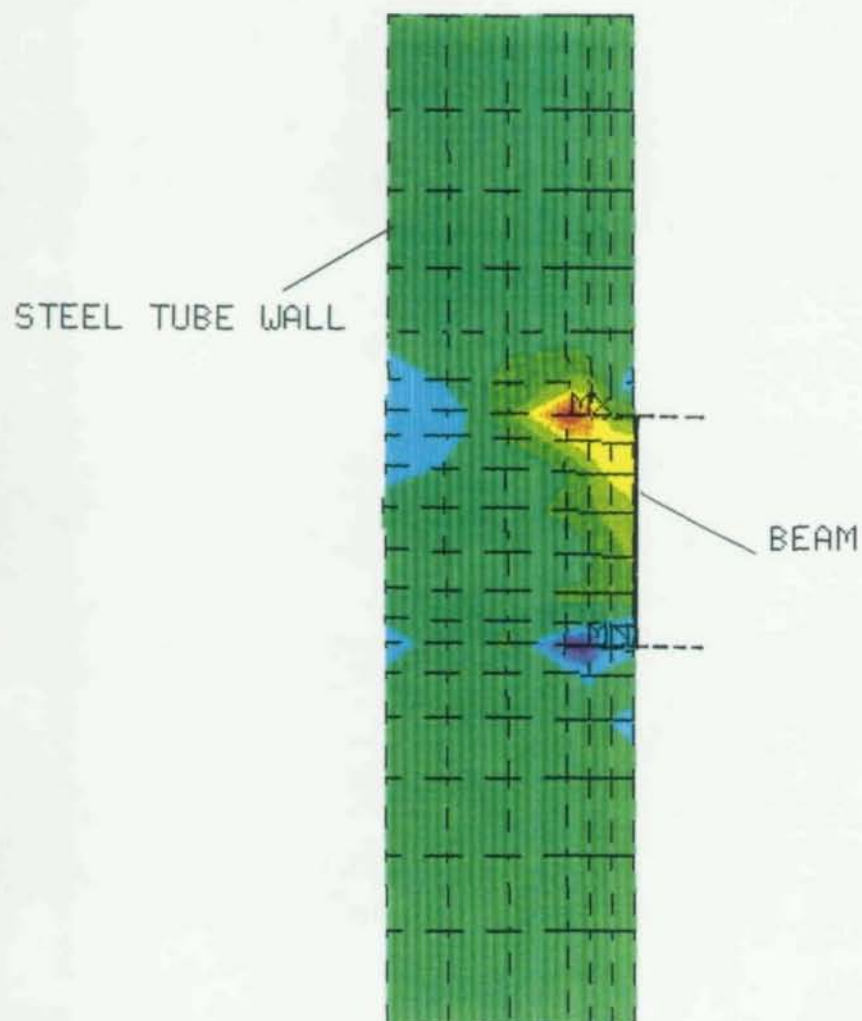
ANSYS 4.4A
AUG 13 1992
21:49:38
POST1 STRESS
STEP=1
ITER=100
SZ   (AVG)
TOP
S GLOBAL
DMX =0.012397
SMN =-4.276
SMX =7.105

XV =1
DIST=71.5
XF =24.605
YF =-65
ZF =-9.84
XRTO=1.63
CENTROID HIDDEN

-4.276
-3.011
-1.746
-0.481972
0.782545
2.047
3.312
4.576
5.841
7.105

Figure 4.10   Horizontal stress distribution in steel tube
              to which beam is connected - Through Connection
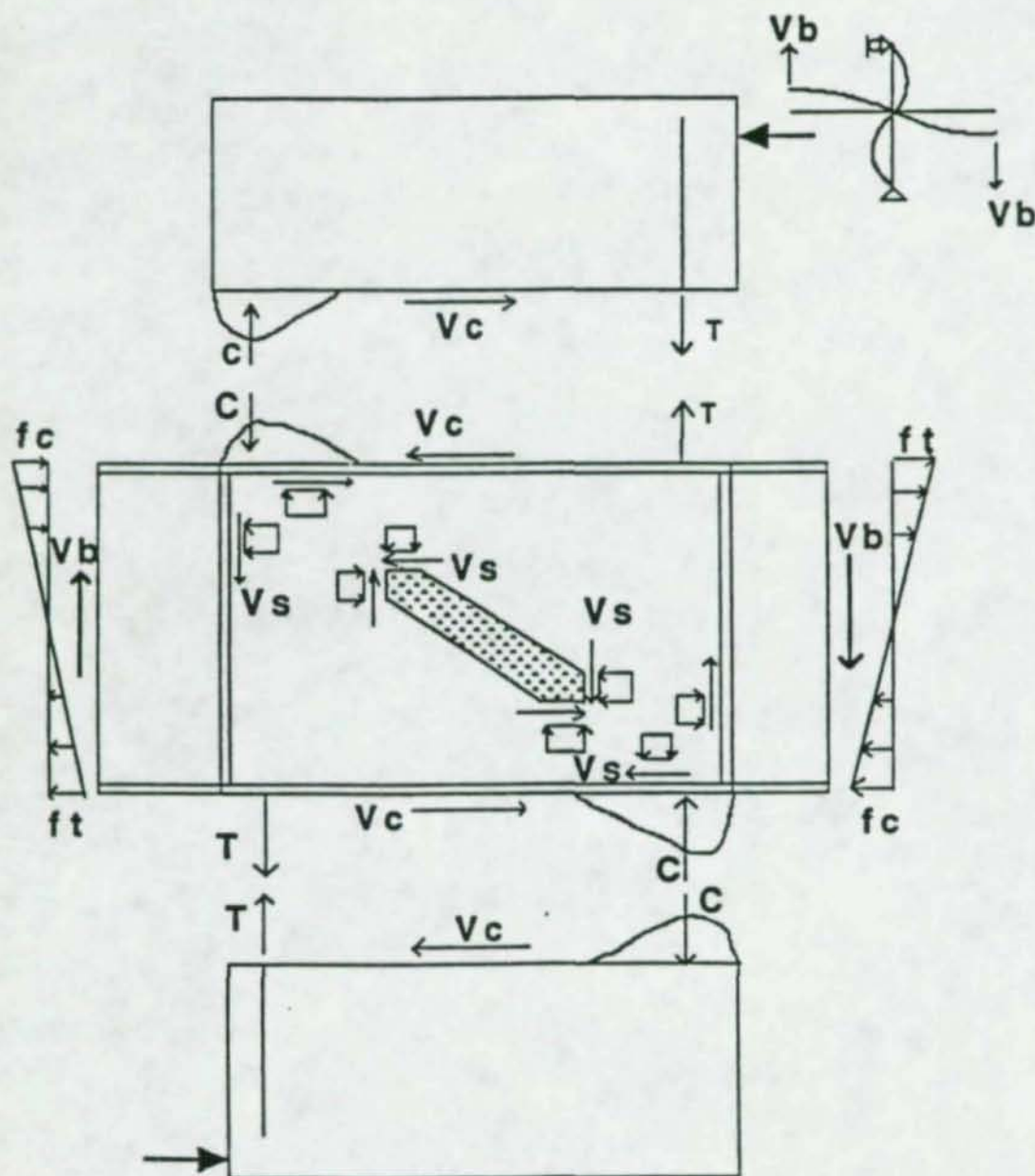
Figure 4.11 Force transfer mechanism in through connection detail

CHAPTER 5

EXPERIMENTAL INVESTIGATION

5.1 General

The experimental program consists of testing an approximately 1/2 scale model of the through connection detail investigated by finite element analysis technique. The steel tube and the beam were fabricated by Valmont Industries Inc. The test specimen was cast and tested at the Structural Engineering Laboratory of University of Nebraska-Lincoln.

5.2 Specimen Description

Figure 5.1, shows the general configuration of the test specimen. The composite column is made up of a 24 in. x 24 in. x 1/2 in. square steel tube filled with concrete. The steel beam is a built-up section and it passes completely through the column. Figure 5.2, shows the different components of the test specimen.

The steel beam is made up of 5/16 in. x 5 1/2 in. flange plates (Grade 50) and a 1/4 in. x 14 in. web plate (A36). This hybrid section is designed such that the beam web within the column reaches shear yield capacity prior to the beam reaching its flexural or shear capacity outside the joint (assuming no contribution from the concrete). The philosophy

54

of forcing failure in the joint is followed for experimental purposes, and is opposite to design practice where preferably failure occurs in the members. As shown in Figure 5.2, four # 11 grade 60 rebars are attached to the beam flanges. Holes were drilled in the beam flanges for passing the rebars, which were later welded to the flanges. These bars transfer a portion of the flange force to the core concrete and prevent the longitudinal movement of beam under cyclic loading. At both ends of the rebars, plates of size 4 in. x 2 in. x 1 in. are welded. These plates are intended to reduce the slip in the rebars. Excessive slip of the rebars could transfer large tensile forces to the steel tube. To provide composite action between steel tube and concrete and to simulate the construction practice, a total of thirty two 3/8 x 2 1/2 inch headed shear studs were welded to two sides of the steel tube where the beam passes through.

5.3 Construction Sequence

The hollow steel tube with I-shaped slot to pass the beam through and the hybrid beam were fabricated by a local firm. As shown in Figure 5.2(a), a cut of size 15 in. x 60 in. and a slot with sufficient clearance to pass the steel beam were made on two opposite faces of the tube. The slot and the cut are made using a torch cut. The edges of the cut plate are bevelled at 45 degrees, so that the plate can be later welded back on to the tube. The cut in the tube wall was made so that the beam and the tube could be instrumented inside the joint region.

Holes were drilled in the beam flanges for attaching #11 vertical rebars. The bars were then welded all around and on both side sides of the flange. Plates of size 2 in. x 4 in. x 1 in., were welded to the rebar end as shown in Figures 5.2 b and c.

Following welding of four # 11 reinforcing bars to the beam flange, necessary instrumentation was done on various components of the connection. Next, a total of 16 shear studs were welded to each 15 x 60 inch portion of the tube that was cut. Sufficient care was taken to see that the instrumentation were not subjected to high temperature developed due to welding. The specimen was cast and cured in a vertical position. Concrete was provided by a local ready mixed concrete company. During casting care was taken to prevent any damage to the instrumentation. A 2 in. diameter penetration type vibrator was used to ensure sufficient compaction of concrete.

5.4 Instrumentation

Strains in the steel elements were measured using strain gages in single and 45 degree rosette configurations. Embedment gages were used to measure the strains in concrete. A total of 37 strain gages and two embedment gages were used. Figures 5.3 to 5.8, show the location of the instrumentation.

Strain gages along the beam flanges measure the axial force distribution in the flange through the joint region. The strain rosettes in the beam web were used to measure the

shear strains in the beam web. The strain rosettes attached to the steel tube measure the bending in the tube wall. The gages attached to the shear studs indicate the stud's participation in transferring horizontal loads. Strain gages were attached to the vertical rebars to measure the axial stresses. Two embedment gages as shown in Figure 5.7 were used to measure the compressive strains along the joint diagonal.

5.5 Material Properties

The static yield stress, ultimate stress, and percentage elongation are reported for the structural steel in Table 5.1. Table 5.2 shows the concrete mix design details. At the time of testing the compressive strength of concrete based on 6 x 12 inch cylinder tests was 14400 psi.

Table 5.1 Material properties for structural steel

Item	Yield stress (psi)	Ultimate stress (psi)	Elongation (%)
Steel tube	42100	64300	26
Beam flanges	65300	80600	23
Beam web	47750	66850	21

Table 5.2 Concrete mix design details

Item	Quantity/cubic yard (lbs)
Fly ash	100
Silica fume	50
Cement	650
Lime stone	1200
C33 sand	300
47B sand	1560
Rheobuild Plasticizer	17
Water	190

5.6 Test Setup and Data Acquisition

Figure 5.9, shows a photograph of the test setup. It consisted of two reinforced concrete

reaction blocks post-tensioned to the lab floor, with the specimen positioned in the middle

of the two blocks. The two reaction blocks provided a means of reacting the column

forces and applied load to the beam ends. Two 60 ton capacity hydraulic rams activated

using a single pump were used to apply equal and opposite loads to the beam ends. Roller supports capable of rotation and horizontal movement were provided at points of support for the columns and the points of load application at beam ends.

The data from the load cells, LVDT's, potentiometers, and strain gages were processed using a HP data acquisition system. During the test, the deflection at one end of the beam was continuously plotted against the load at that end using an X-Y plotter. Prior to testing the entire test setup was white washed with lime.

5.7 Testing Procedure

Before starting the actual test, the specimen was subjected to very low levels of load several times. This was done to make sure that all the instrumentation and the test setup were functioning properly.

The test specimen was subjected to monotonic lateral loading only. No axial load was applied on column. The load was applied in small increments. Data was collected at each load step after waiting for 5 to 10 minutes for the structure to reach steady state equilibrium. Loading was terminated on one side of the beam when it exhibited large web buckling outside the joint region. After this stage the specimen was unloaded. Loading was continued on the other end of the beam until it failed by web buckling outside the joint region.

5.8 Experimental Results

The general behavior of the test specimen is described using the strain data obtained from various gages attached to the specimen. Only the data from gages which functioned properly during testing are presented.

Figure 5.10, shows a plot of average applied load versus average beam deflection. Loads corresponding to nominal yield and plastic moment capacities of the beam cross-section are also shown in Figure 5.10. The beam started to exhibit nonlinear load-deflection characteristics at a displacement of approximately 0.2 inches which corresponds to 0.43% story drift. Maximum applied beam load was reached at approximately 0.4 inches of beam displacement corresponding to 0.86% story drift. Maximum beam deflection of approximately 0.7 inches was observed when the beam on one side of the column outside the joint region exhibited web buckling. This displacement corresponds to 1.5% story drift. At this stage no visible damage or yielding of the steel tube were noticed.

Figure 5.11, shows a plot of the longitudinal strain distribution in the beam flange. The flange strains inside the joint region are much lower than those outside the joint. The strains in gages 2, 3 and 5 reached their maximums at about 0.4 inches of beam deflection and remained constant thereafter, while the strain in the gage located outside the joint (gage 1) continued to increase rapidly.

Figures 5.12 to 5.14 show the strain distribution in beam web. Also shown in Figure 5.12 is the direction of the applied loads and two lines, GG and HH, which connect the corners of the web within the joint. The information shown in Figures 5.12 indicate that the beam web within the joint is subjected primarily to tensile and compressive strains along the lines GG and HH, respectively. This type of deformation indicates that the beam web experiences shear type of deformation.

It can also be observed from Figure 5.12, that the tensile strains along lines parallel to line GG are significantly higher than compressive strains along lines parallel to the line HH. This behavior can be explained as follows. The type of shear deformation imposed on the beam web within the joint results in activating a concrete compression strut parallel to line HH. This compression strut acts as a stiffener along the diagonal HH, thereby reducing the compressive strain in the beam web along that direction. However, along line GG, tensile strain in the beam web increases since the concrete is not effective. This observation verifies the force transfer deduced from analytical investigation as explained earlier.

Figure 5.15, shows the data from the strain gages attached to one of the vertical steel rods. Gage data from gages 23 and 24, show that there is a sudden increase in strain in the steel rod at approximately 0.08 inches of beam deflection. This behavior could be associated with cracking of concrete in the vicinity of the rod and subsequent transfer of tensile stresses from the concrete to the rod. Data from these gages could also be

correlated to strain data obtained from gages attached to the steel tube and shear studs as shown in Figures 5.16 & 5.17. Gage 22 in Figure 5.15, gages 37-39 in Figure 5.16, and gages 32-33 in Figure 5.17, were all located on the same side of the beam flange. Examination of Figures 5.15 through 5.17 show that the increase in tensile strain in the steel tube is closely related to the stretching of the rod. The sudden increase in steel rod strain at the beam displacement of 0.08 inches also coincides with the sudden increase of tensile strain in the steel tube and shear studs. Further, once the steel rod exhibits constant strain level (Figure 5.15), the strain in steel tube (Figure 5.16) exhibits the same behavior. This behavior suggests (1) the need to provide vertical reinforcing rods to control stretching of the steel tube, (2) the need to prevent excessive slip of the reinforcing rods which justifies the idea of mechanical anchorages such as plates welded to the rod ends, and (3) the need to prevent excessive elongation of reinforcing rods by basing their design on stiffness rather than strength considerations.

5.9 Conclusions from Experimental Investigation

The results obtained from the experiment indicates the formation of concrete compression strut in the joint region, thus verifying the force transfer mechanism deduced from finite element analyses. The experiment also proved that the reinforcing rods attached to the beam flanges within the joint will reduce the stress transfer to the steel tube.
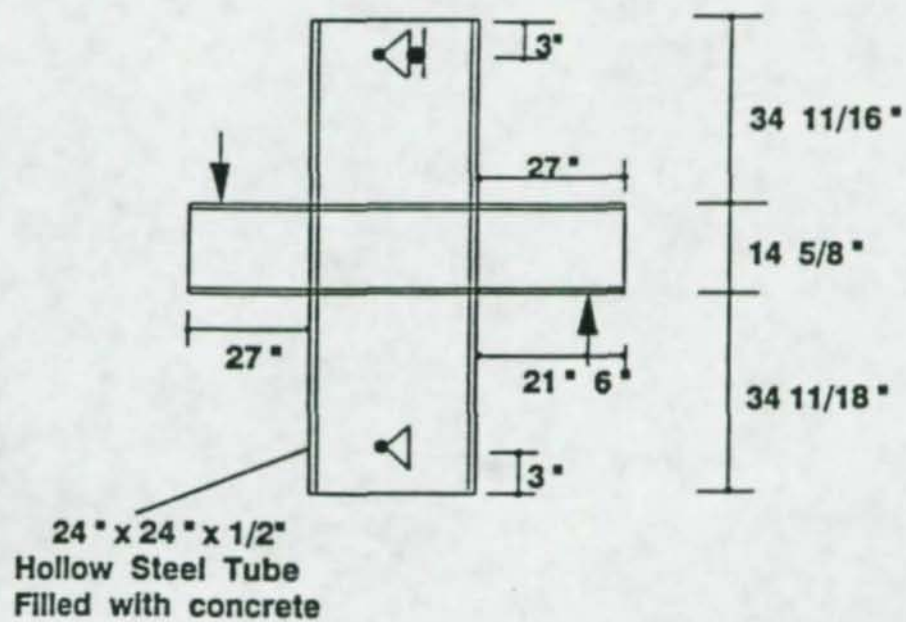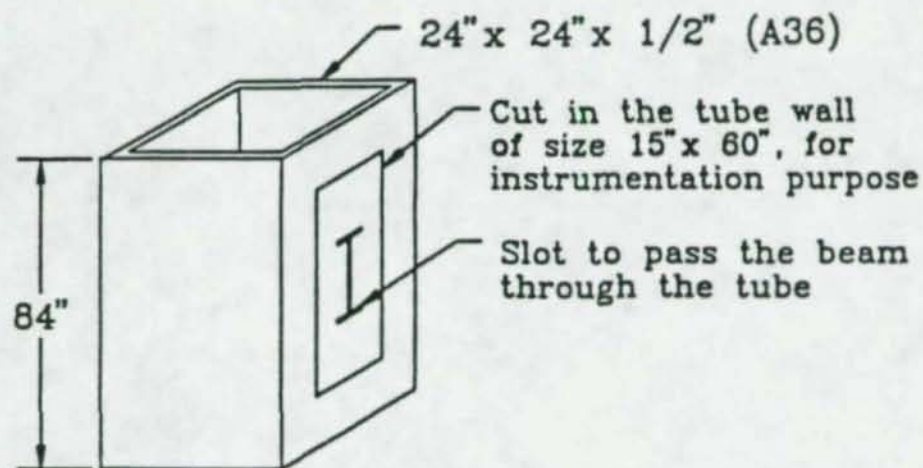
63

24 " x 24 " x 1/2"
Hollow Steel Tube
Filled with concrete

Figure 5.1   General configuration of the test specimen

24" x 24" x 1/2" (A36)

Cut in the tube wall
of size 15" x 60", for
instrumentation purpose

Slot to pass the beam
through the tube

84"

(a)

ℓ 4" x 2" x 1"

#11 Rebar

$3\frac{1}{2}$"

15"

$5\frac{1}{2}$" x $\frac{5}{16}$" (GR50)

14" x $\frac{1}{4}$" (A36)

$5\frac{1}{2}$" x $\frac{5}{16}$" (GR50)

15"

$\frac{1}{4}$

A

A

18"

78"

Section A–A

(c)

(b)
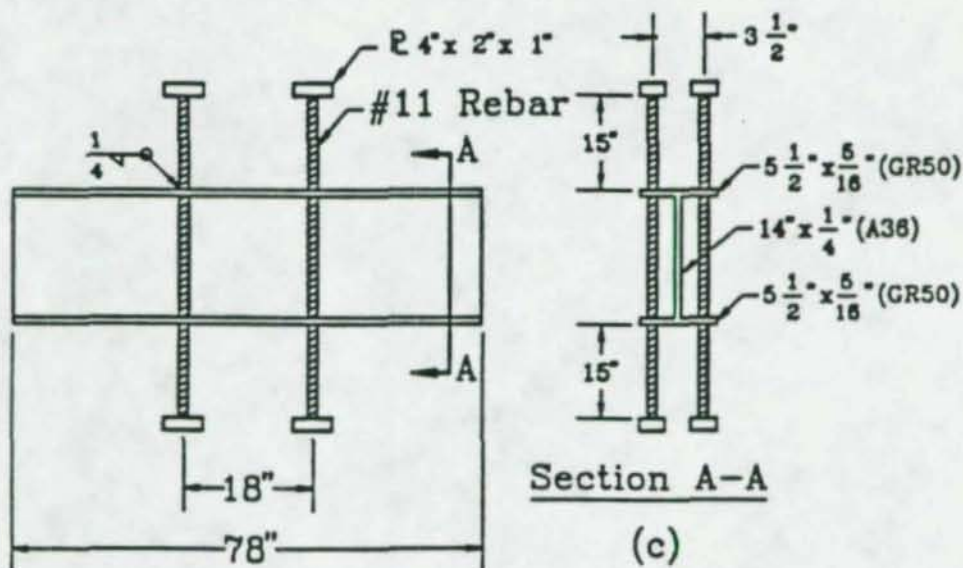
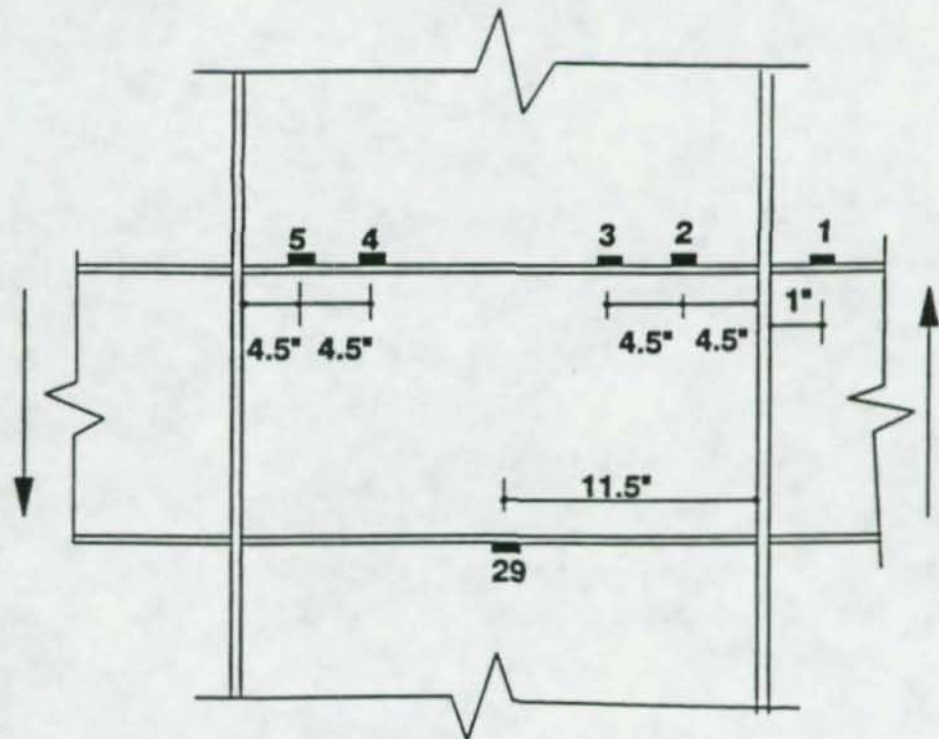Figure 5.2   Different components of the test specimen

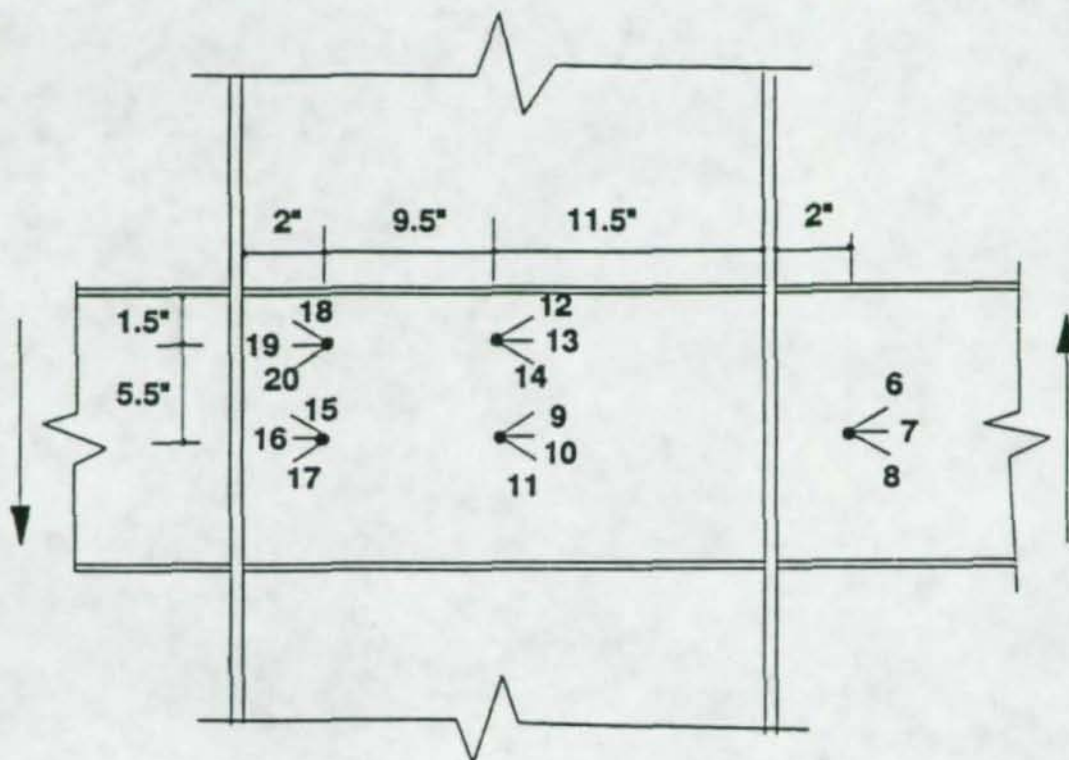Figure 5.3   Strain gage locations on the beam flange

Figure 5.4   Strain gage locations on the beam web
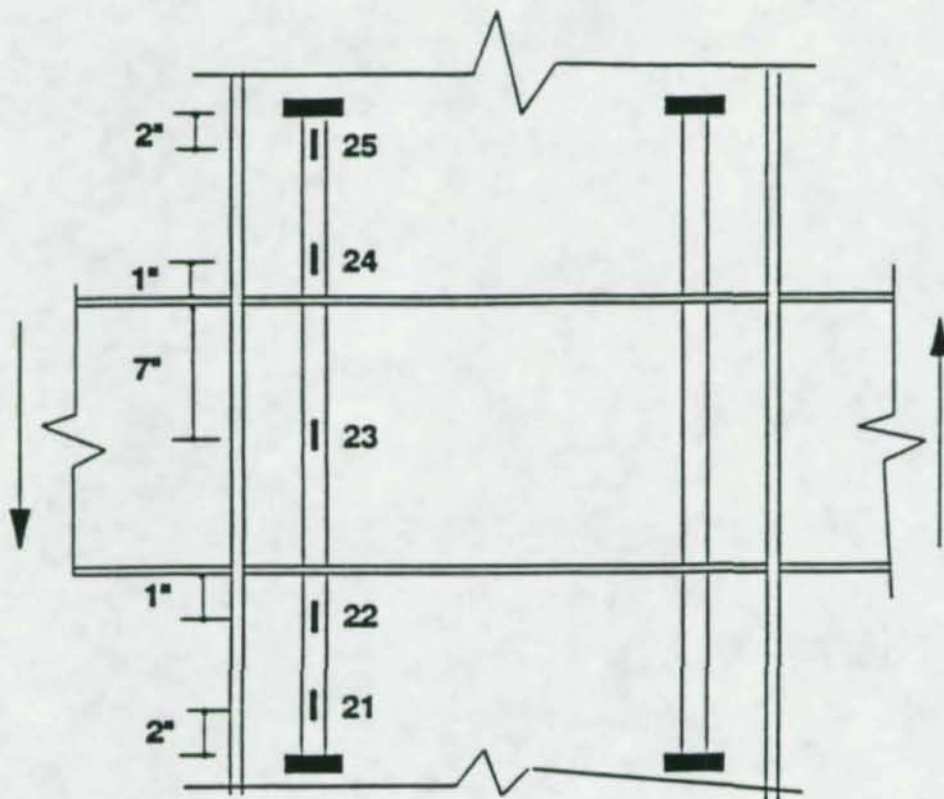
Figure 5.5   Strain gage locations on the vertical reinforcing bar
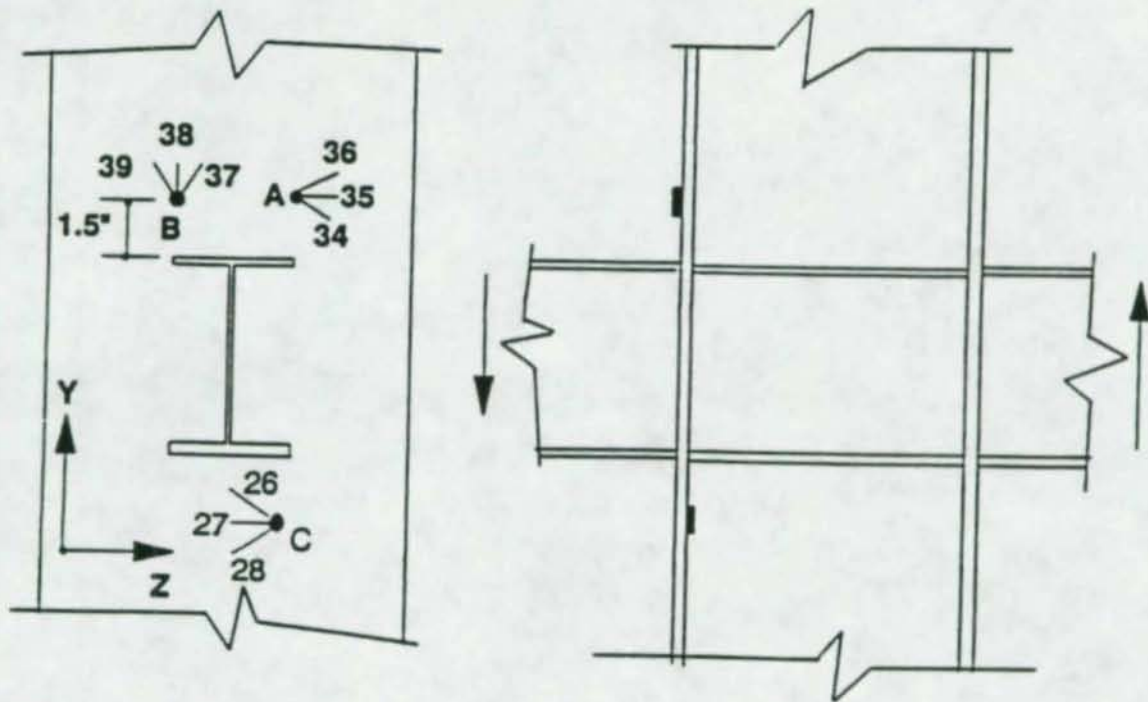
Figure 5.6   Strain gage locations on the steel tube wall
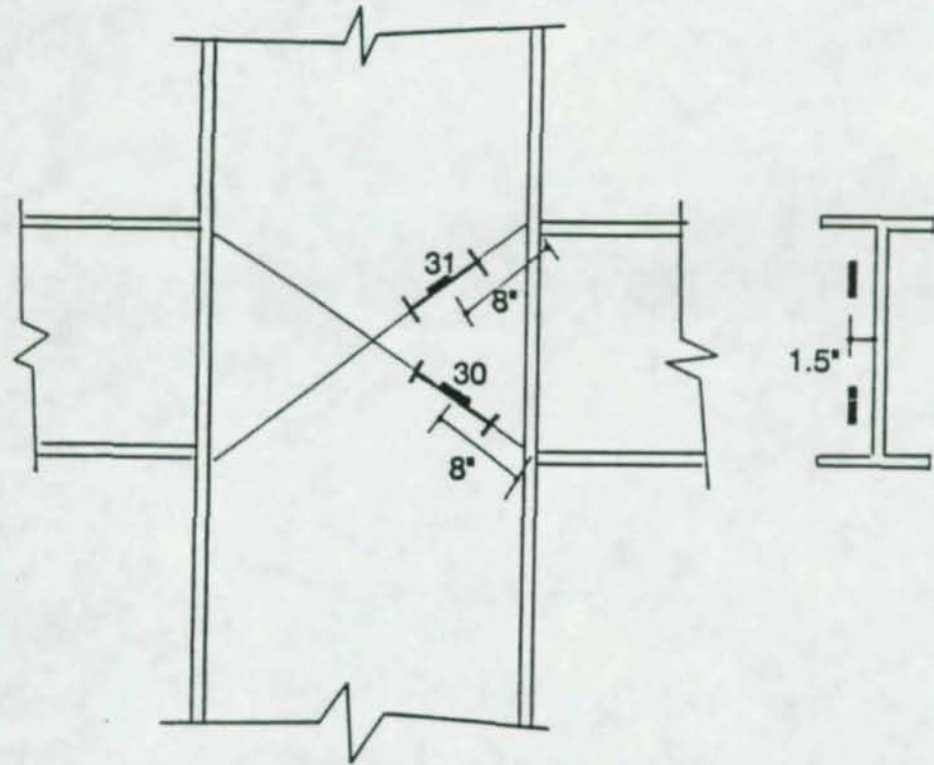
Figure 5.7   Embedment gage locations
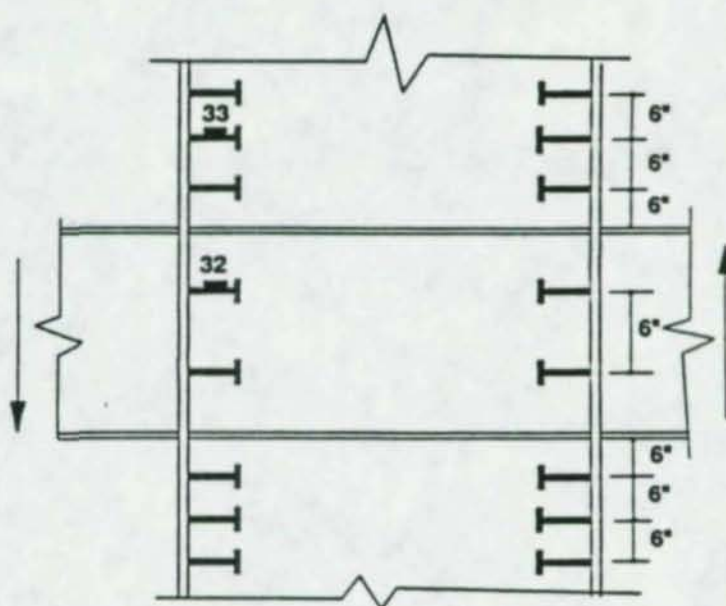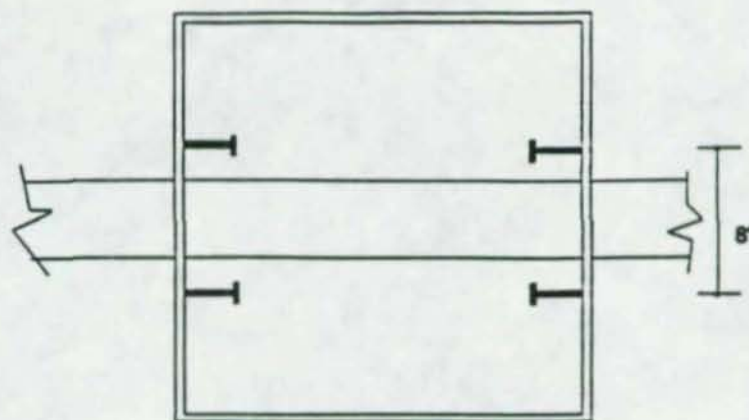
Figure 5.8   Strain gage locations on the shear studs
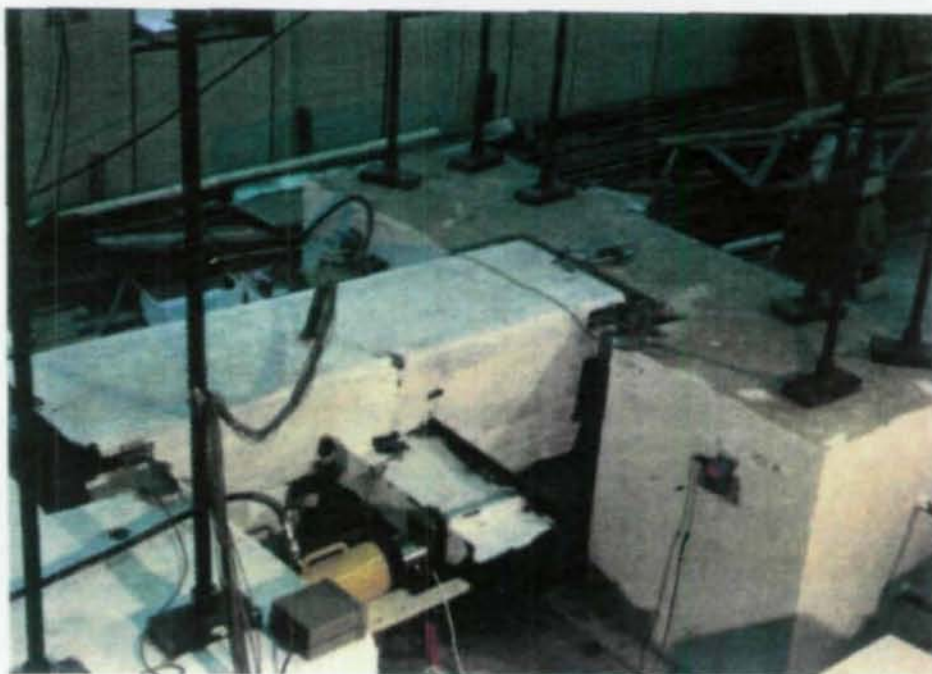
Figure 5.9 Photograph of the test set-up
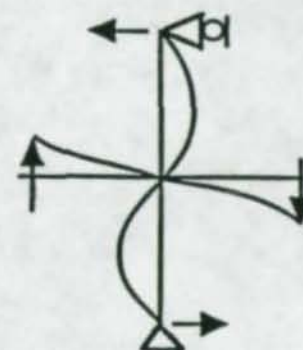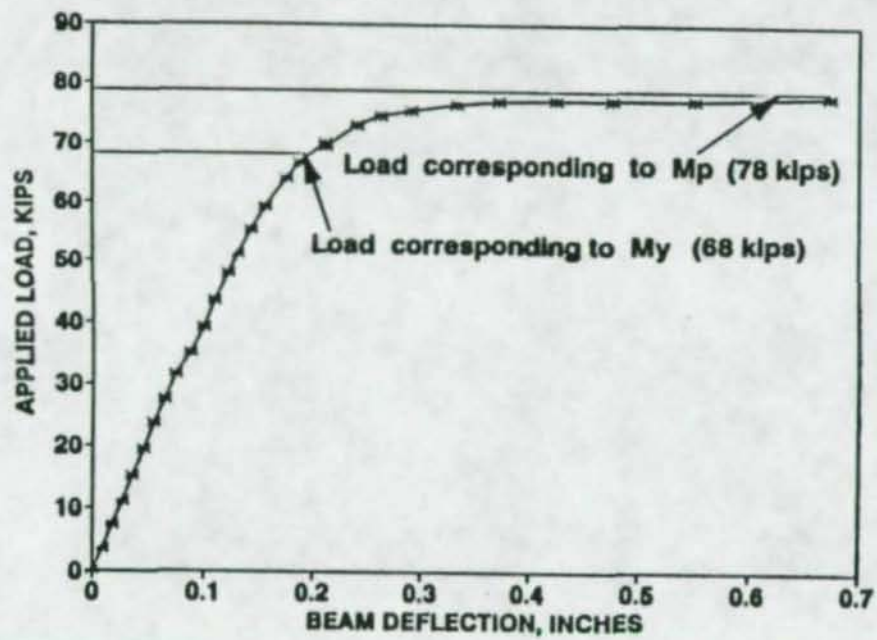
Figure 5.10   Load-deflection plot
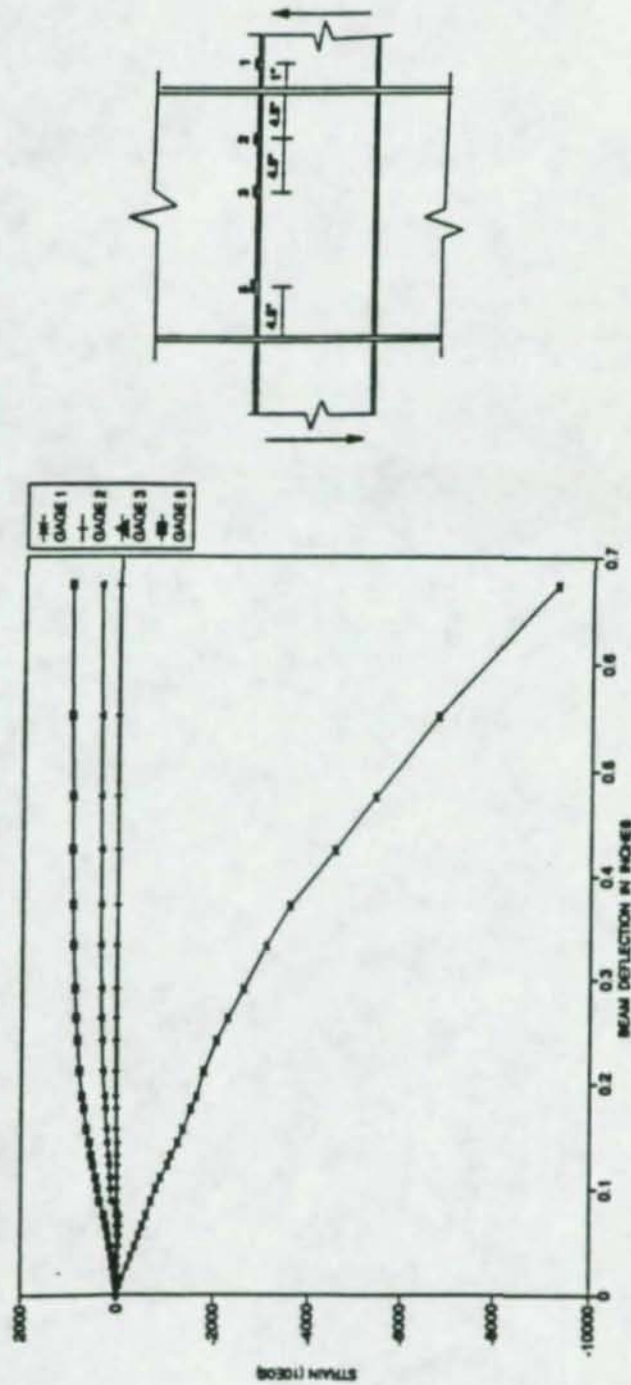
Figure 5.11   Longitudinal strain distribution in the beam flange
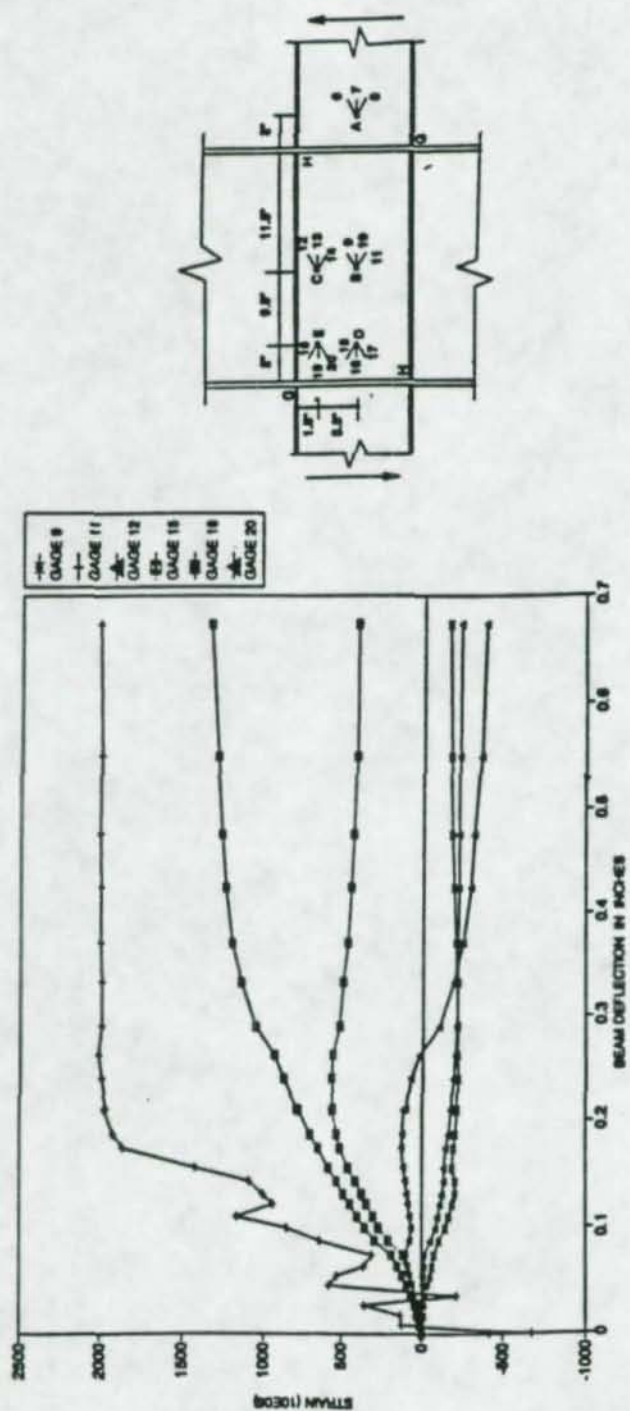
Figure 5.12   Strain distribution in the beam web
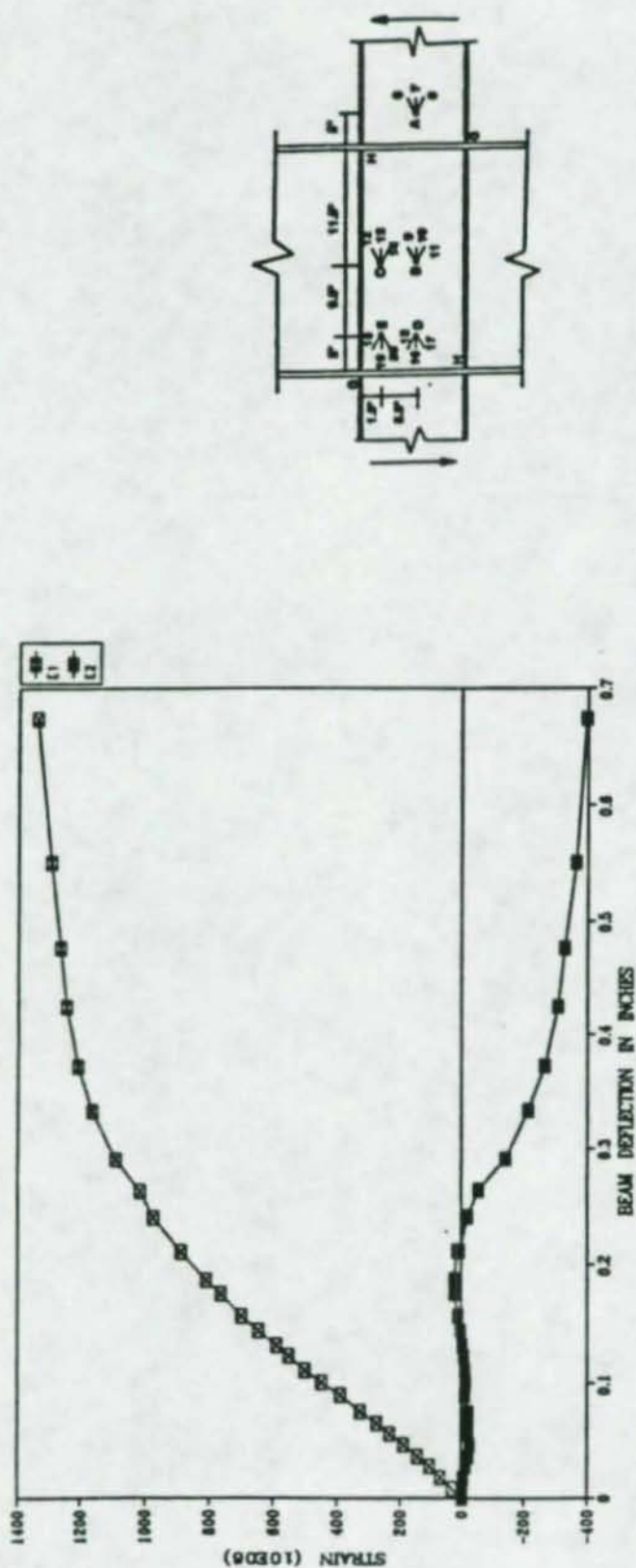
Figure 5.13   Maximum and Minimum Principal strains in the beam web at B
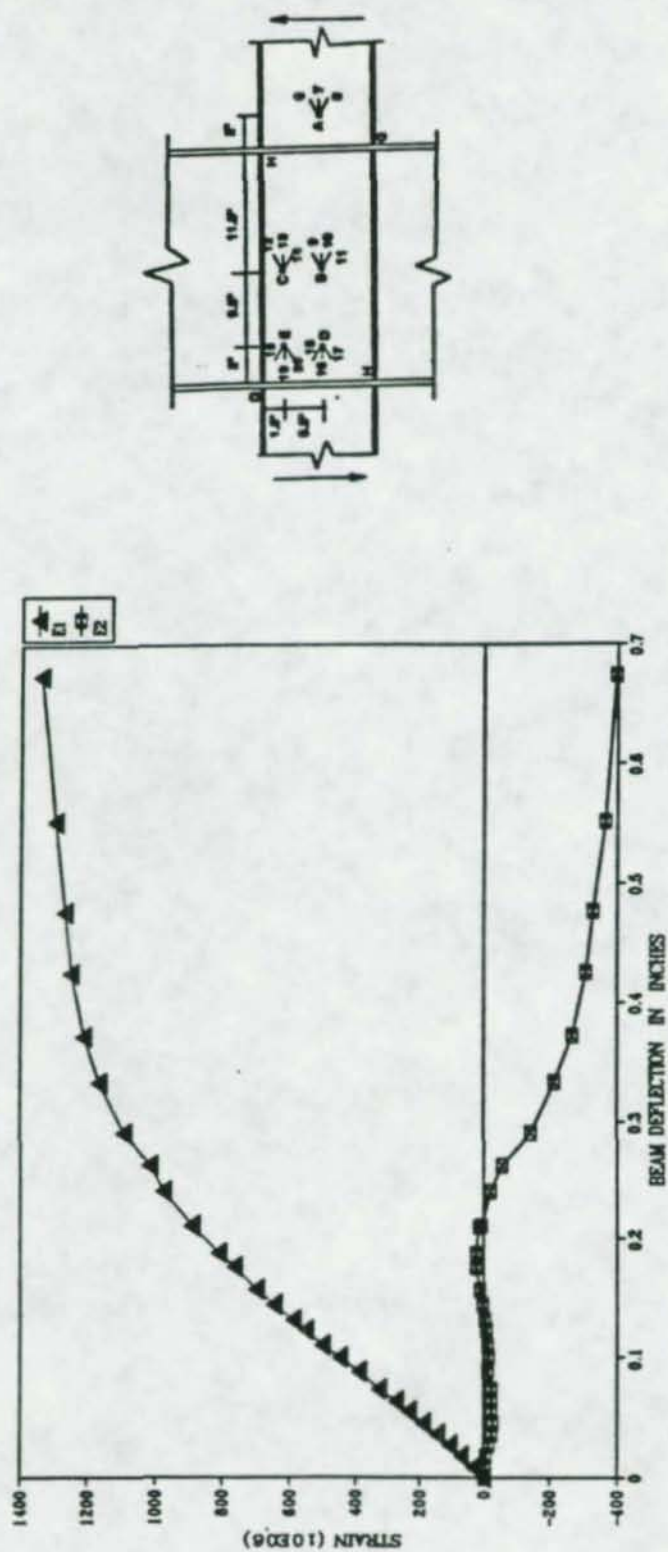
Figure 5.14   Maximum and Minimum Principal strains in the beam web at E
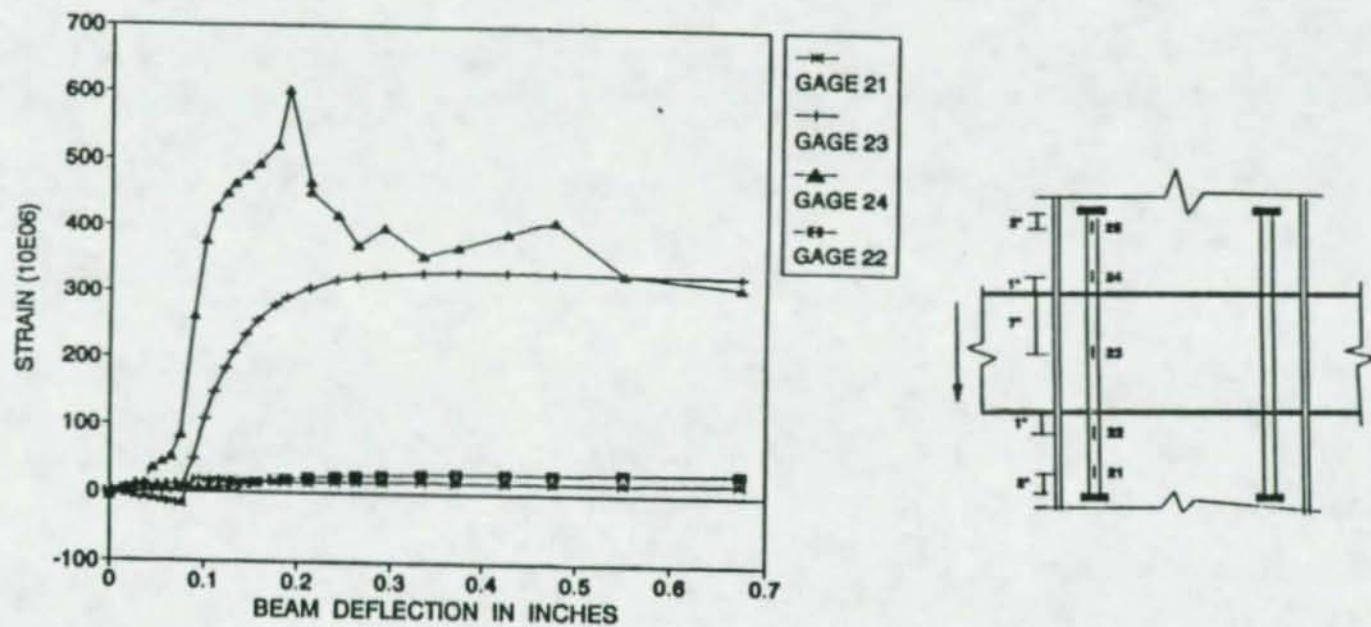
Figure 5.15   Strain distribution in the vertical reinforcing bar
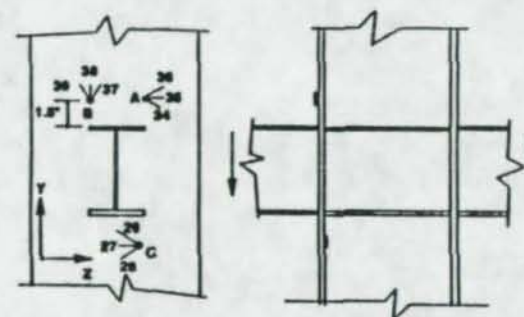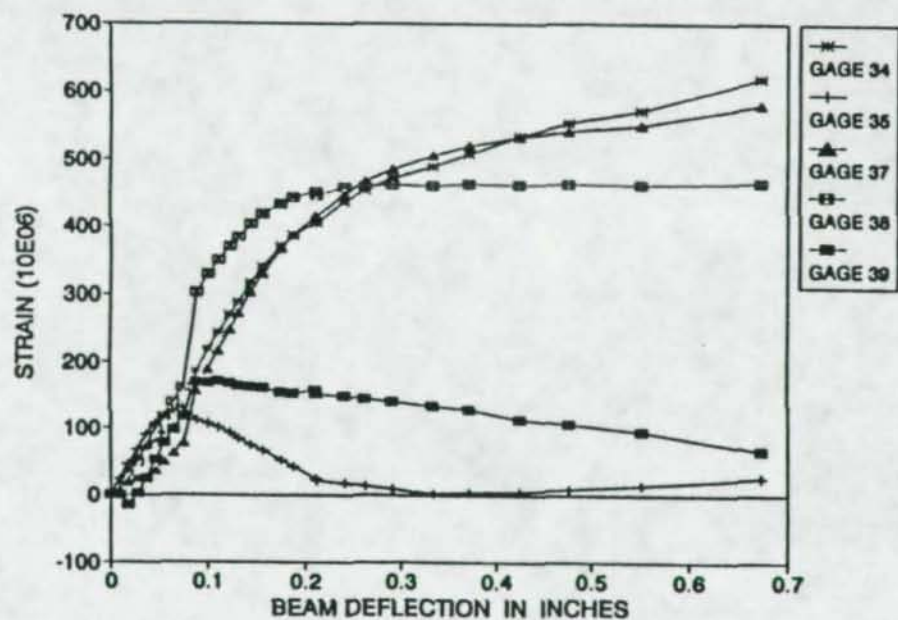
Figure 5.16   Strain distribution in the steel tube wall
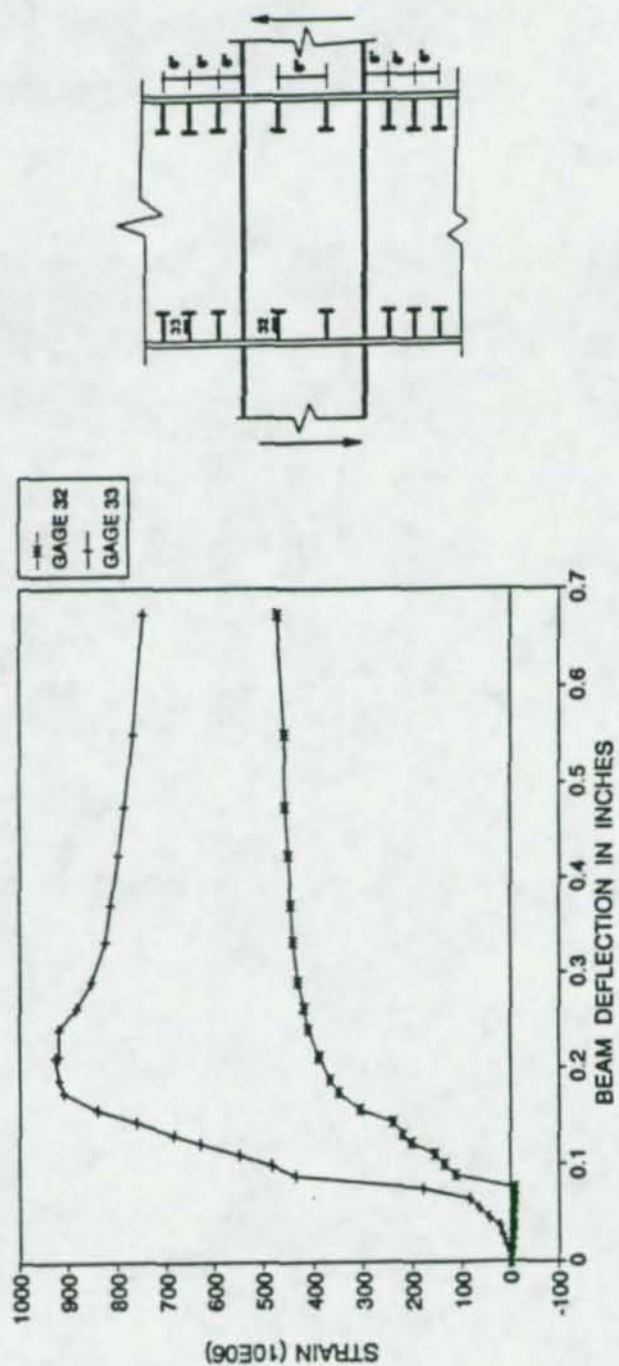
Figure 5.17 Strain distribution in the shear studs

CHAPTER 6

BEHAVIORAL MODEL AND DESIGN APPROACH

6.1 General

This chapter presents the details of developing a behavioral model and design approach for the through connection detail. Results from finite element analyses and experimental work are used to develop equations which relates the applied external forces on the connection to the internal forces developed in the connection. Making use of these equations, a design approach for through connection detail is presented.

6.2 Behavioral Model

based on results of the finite element analysis and experimental results, a behavioral model in the form of equations relating the applied external forces to the connection's internal forces was developed. These equations are then used to suggest a tentative design criteria for through beam connection detail.

In developing the behavioral model the following assumptions were made:

(a)   Externally applied shear forces and moment at the joint are known

(b)   Failure is defined as the point at which the beam web within the joint reaches its shear stress limit when externally applied forces are at their ultimate values

(c)   At failure the concrete stress distribution is linear and maximum concrete compressive stress is below its limiting value.

The joint forces implied in assumption (a) could be obtained from analysis and requires the knowledge of applied shear and moment at the joint at failure. These quantities are assumed to be related as follows:

$$V_c = \alpha \ V_b$$

$$M_b = l_1 \ V_b$$

$$M_c = l_2 \ V_c$$

where V_b and M_b are ultimate beam shear and moment, respectively, while V_c and M_c are ultimate column shear and moment, respectively. Figure 6.1, shows these forces for an isolated portion of a structure subjected to lateral loads.

The validity of assumption (c) above could be justified for the following reasons:

(i) Column sizes for the type of construction considered in this study are generally much larger than the beam sizes and

(ii) The concrete type used in these columns is generally high strength concrete with compressive strength well above 10000 psi. The uniaxial stress-strain characteristics of high strength concrete exhibits a linear behavior up to maximum strength, followed by a sharp descending portion.

6.3 Derivation of Behavioral Model

The type of joint is shown in Figure 6.1. Figure 6.2 shows the Free Body Diagram (FBD) of the beam web within the joint and upper column at ultimate load. With reference to Figure 6.2, the following additional assumptions are made in deriving the behavioral model:

(1) The concrete stress distribution is assumed to be linear. The width of the concrete stress block is assumed to be equal to b_f, the beam flange width

(2) As shown in Figure 6.2 strain distribution over the upper column is assumed to be linear

(3) The steel tube and concrete act compositely

(4) The portion of the upper column shear, V_c, transferred to the steel beam is assumed to be βC_c, where C_c is the resultant concrete compressive force bearing against the beam flange and β is the coefficient of friction

(5) Applied beam moments are resolved in to couples concentrated at beam flanges

(6) Resultant of concrete compression strut is along a diagonal as shown in Figure 6.2.

Considering the above assumptions and strain distribution shown for the upper column in Figure 6.2, strain for different connection elements could be related to ϵ_l, steel tube strain in tension.

$$\epsilon_c = \frac{a}{d_c - a} \epsilon_l \qquad (6.1)$$

$$\epsilon_{sc} = \frac{a - d_1}{d_c - a} \epsilon_l \qquad (6.2)$$

$$\epsilon_{st} = \frac{d_c - d_1 - a}{d_c - a} \epsilon_l \qquad (6.3)$$

where ϵ_c = maximum compressive strain in steel tube and concrete

ϵ_{sc} = compressive strain in steel rod

ϵ_{st} = tensile strain in steel rod

Next, maximum stresses in concrete and stresses in the steel tube could be calculated as follows:

$$f_c = E_c \epsilon_c \qquad (6.4)$$

$$f_{sc} = E_s \epsilon_{sc} \qquad (6.5)$$

$$f_{lc} = E_s \epsilon_c \qquad (6.6)$$

$$f_{st} = E_s \epsilon_{st} \qquad (6.7)$$

$$f_{lt} = E_s \epsilon_l \qquad (6.8)$$

where f_c = maximum concrete compressive stress

$$f_{sc} = \text{compressive stress in steel rod}$$

$$f_{lc} = \text{compressive stress in steel tube}$$

$$f_{st} = \text{tensile stress in steel rod}$$

$$f_{lt} = \text{tensile stress in steel tube}$$

Substituting equations 6.1 through 6.3 in equations 6.4 through 6.8 and multiplying equations 6.4 through 6.8 by corresponding area, the resultant forces for different connection elements could be calculated as follows:

$$C_c = 1/2 \ \eta \ \xi \ b_f \ \frac{a^2}{d_c - a} \ f_{yl} \tag{6.9}$$

$$C_l = \gamma \ \xi \ b_f \ t_l \ \frac{a}{d_c - a} \ f_{yl} \tag{6.10}$$

$$C_s = A_s \ \xi \ \frac{a - d_1}{d_c - a} \ f_{yl} \tag{6.11}$$

$$T_s = A_s \ \xi \ \frac{d_c - d_1 - a}{d_c - a} \ f_{yl} \tag{6.12}$$

$$T_l = \xi \ \gamma \ b_f \ t_l \ f_{yl} \tag{6.13}$$

Using the FBD of the upper column shown in Figure 6.2, equations 6.9 through 6.13, and satisfying vertical force equilibrium, the following equation could be obtained.

$$A_s = \frac{1}{d_c - 2a} [\ 1/2\ \eta\ b_f\ a^2 - A_l\ (d_c - 2a)\ ] \qquad (6.14)$$

where b_f =   beam flange width

        d_c =   depth of column

        a =   depth of concrete compression block

        η =   ratio of modulus of elasticity for concrete over modulus of elasticity of

            steel

        A_l =   effective area of steel tube = $2\ b_f\ t_l$

        A_s =   area of steel rod at each corner of beam

        t_l =   thickness of steel tube wall

In defining A_l it is assumed that a steel tube width equal to two times the beam flange width is effective in carrying tension and compression. This value was estimated from experimental results.

Next, considering the moment equilibrium of the FBD of the upper column shown in Figure 6.2, the following expression can be derived.

$$V_b = [A_l\ ad_c + A_s(ad_c - 2d_l d_c + 2d_l^2) + 1/2\ \eta\ b_f\ a^2(d_c - a/3)]\frac{\xi\ f_{yl}}{\alpha\ l_2(d_c - a)} \qquad (6.15)$$

where d_l =   distance between steel rod and steel tube

        f_{yl} =   yield strength of steel tube

In equation 6.15, ξf_{yl} is the stress level to which the steel tube is allowed to approach at ultimate condition. ξf_{yl} could also be viewed as the portion of the steel tube strength utilized to resist the forces transferred by the connection. Based on the limited experimental data obtained from this investigation it is suggested that a value of 0.35 be used for ξ.

Equations 6.14 and 6.15 relate the externally applied force, V_b, directly and the externally applied forces V_c and M_c indirectly (through the coefficients α and l_2) to different connection parameters such as A_s, A_t, and a.

6.4 Design Approach

Before proceeding with the steps necessary in designing the through beam connection detail, additional equations will be derived to relate the shear stress in the beam web within the joint to the compressive force in the compression strut and externally applied forces.

Considering the FBD of the portion of beam web within the joint area as shown in Figure 6.3 and satisfying the horizontal force equilibrium, the following equation could be derived:

$$V_w + C_{st} \cos\theta + \beta\, C_c - \frac{2\, M_b}{d_b} = 0 \qquad\qquad (6.16)$$

where V_w =   shear force in the beam web at ultimate condition

        C_{st} =   compressive force in the concrete compression strut

        θ = $\arctan(d_b/d_c)$

Equations 6.14 through 6.16 could be used to proportion the through connection detail.

Until further research is conducted the following steps are suggested for designing the through beam connection detail following the LRFD format.

    step 1.   From analysis obtain the factored joint forces

    step 2.   Select the following quantities: t_i, b_f, d_b, d_c, d_1, f_{yl}

    step 3.   Solving equations 6.14 and 6.15 simultaneously, obtain A_s and a. This can be

               achieved using a trial and error approach.

    step 4.   Check the stresses in different connection elements

    step 5.   Assuming that the beam web yields at ultimate load. With this assumption V_w

               could be calculated as follows:

$$V_w = 0.6\, F_{yw}\, t_w\, d_c \qquad\qquad (6.17)$$

where, F_{yw} = beam web yield stress and t_w = beam web thickness

step 6. Using equation 6.16 calculate C_{st}, compressive force in the concrete compression strut, and applied shear force to the concrete in the joint area

step 7. Check shear stress in concrete in the joint area. The limiting shear force could be assumed to be as suggested by ACI 352 as:

$$V_u = \phi \, R \, \sqrt{f'_c} \, A_e \qquad\qquad (6.18)$$

where,

$\Phi = 0.85$

$R = 20, 15,$ and 12 for interior, exterior, and corner joints, respectively

$f'_c =$ concrete compressive strength

It is suggested that the value of $\sqrt{f'_c}$ be limited to 100 psi, implying that in case of 15000 psi concrete, $\sqrt{f'_c}$ be taken as 100 rather than 122 as it would be. Also, until further research is conducted it is suggested to calculate A_e as below:

$A_e = 2 \, b_f \, d_c$

6.5 Design Example

Design a through beam connection detail with the following geometry and properties.

Given (steps 1 and 2):

$t_1 = 0.5$ inch

$b_f = 5.5$ inch

$d_b = 14.5$ inch

d_c = 24.0 inch

d_1 = 3.5 inch

t_w = 0.25 inch

l_2 = 32 inch

A_l = 5.5 inch^2

V_b = 79 kips

M_b = 1660 inch-kips

f_{yl} = 36 ksi

F_{yw} = 36 ksi

f'_c = 14 ksi

E_s = 29000 ksi (modulus of elasticity of steel)

E_c = 6670 ksi (modulus of elasticity of concrete)

α = 0.85

β = 0.5

ξ = 0.35

η = 0.23

Step 3.   Using a trial and error approach and equations 6.14 and 6.15, calculate

a and A_s. For the first trial assume a = 8.5 inch. Equation 6.14 will

result in:

$$A_s = \frac{1}{24 - 2*8.5}[1/2*0.23*5.5*8.5^2 - 5.5*(24 - 2*8.5)]$$

$$A_s = 1.03 \text{ inch}^2$$

Substitute $A_s = 1.03$ inch^2 in equation 6.15 and calculate V_b. If the result

is approximately equal to 79 kips, then the assumed value of a is o.k.

Equation 6.15 yields:

$V_b = 64.3$ kips $\neq 79$ kips.

For the second trial assume a = 9 inches. This will yield $A_s = 3.04$

inch^2, and $V_b = 77$ kips $\simeq 79$ kips o.k.

Therefore, a = 9 inches and $A_s = 3.04$ inch^2.

Use 2-#11 Grade 60 deformed reinforcing bars $A_s = 3.12$ inch^2

Step 4. Check stresses in different connection elements against their limit values.

First calculate tensile strain in steel tube.

$\epsilon_l = (\xi\ f_{yl})/E_s = 0.35*36/29000 = 0.000434$ inch/inch

Using equations 6.1 and 6.4 calculate f_c.

$f_c = 1.74$ ksi $< f'_c = 14$ ksi o.k.

Using equations 6.2, 6.3, 6.5, 6.6, 6.7, and 6.8 calculate stresses in other

connection elements. This yields:

$f_{sc} = 4.61$ ksi $< \Phi_c\ F_y = 0.85 * 60 = 51$ ksi   o.k.

$f_{lc} = 7.55$ ksi $< \Phi_c\ F_y = 0.85 * 36 = 30.6$ ksi   o.k.

$f_{st} = 9.65$ ksi $< \Phi_l\ F_y = 0.90 * 60 = 54$ ksi   o.k.

$f_{lt} = 12.6$ ksi $< \Phi_l\ F_y = 0.90 * 36 = 32.4$ ksi   o.k.

Step 5: Using equation 6.17, calculate shear force in the beam web.

$V_w = 0.6 * 36 * 0.25 * 24 = 129.6$ kips

Step 6:   Using equation 6.16 calculate compressive force in concrete compression

strut.

θ =arctan (14.5/24) = 31.1°

$C_c = 1/2 * 0.23 * 0.35 * 5.5 *(9^2/24 - 9) * 36 = 43$ kips

$V_w + C_{st} Cos(\theta) + \beta C_c - (2M_b/d_b) = 0$

$129.6 + C_{st} \cos(31.1) + 0.5(43) - (2*1660)/14.5 = 0$

$C_{st} = 90.9$ kips

Step 7:   The shear force carried by concrete within the joint between the beam

flanges is assumed to be the horizontal component, C_{st}.

$V_c = C_{st} = Cos(\theta) = 90.9 \cos(31.1) = 77.8$ kips

For the interior joint the shear capacity is $V_u = \Phi (20) f'_c (2b_f)(d_c)$

$V_u = 0.85 (20) 100 [(2*5.5) (24)]/1000 = 449$ kips > 77.8 kips   o.k.

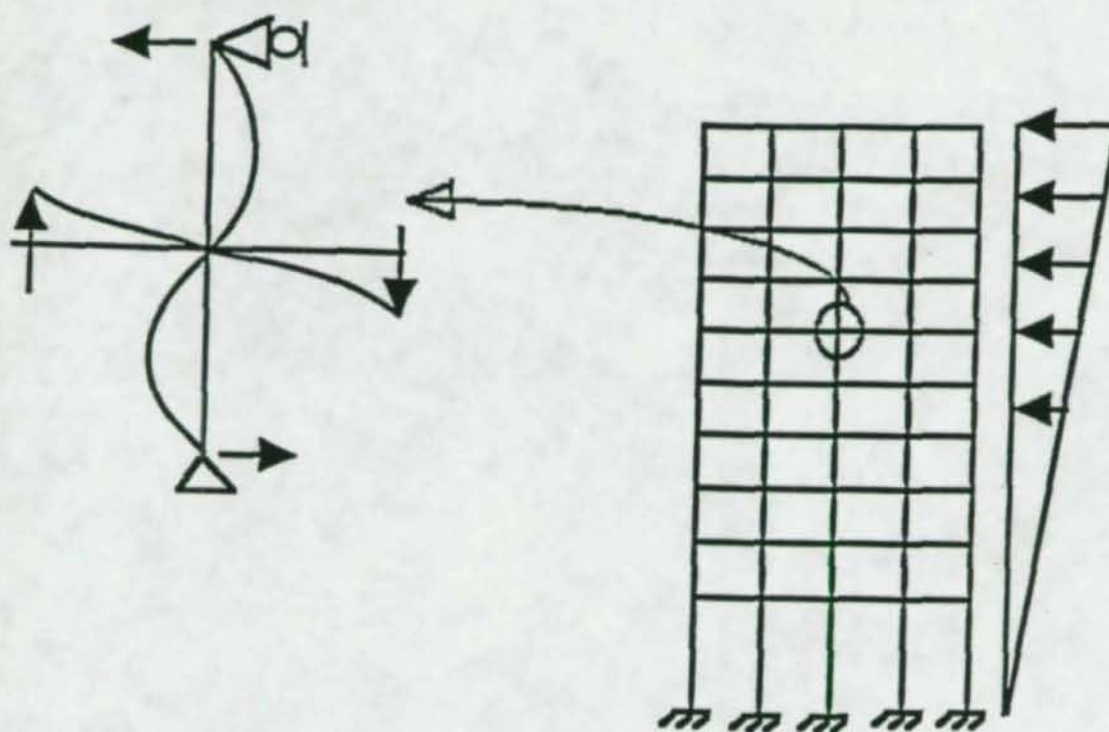This completes the design of through connection detail for the given data.

Figure 6.1   Assumed forces on an interior joint in a frame subjected to lateral loads
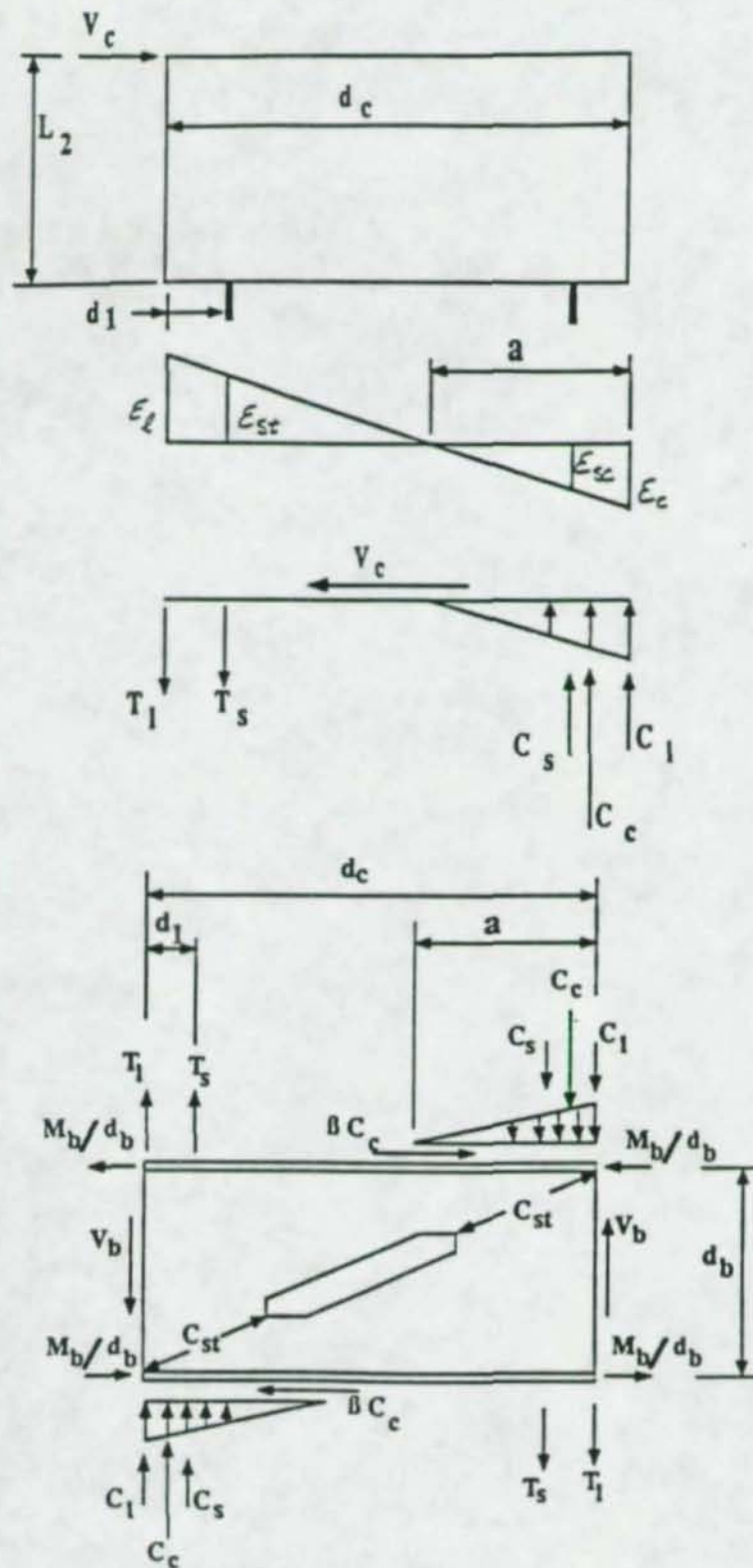
93

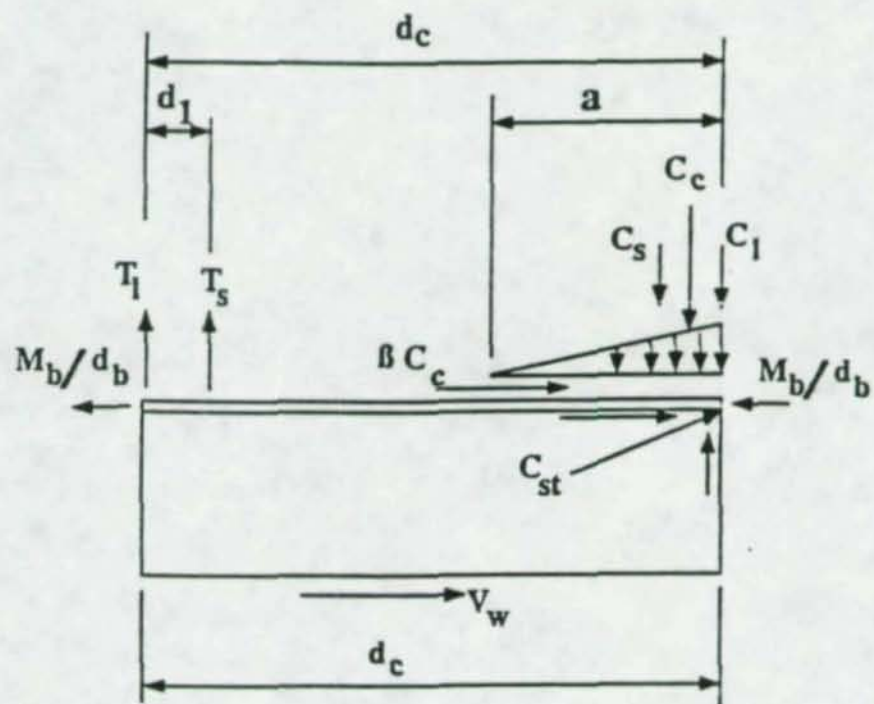Figure 6.2   FBD of the upper column and beam web within the joint area

Figure 6.3 FBD of the portion of the web within the joint area

CHAPTER 7

CONCLUSIONS

7.1 Conclusions

The use of composite column columns of the type described in this report is proven to be economical. This report has summarized a suggested connection detail (a through beam connection detail) for connecting steel beams to these columns as well as tentative design guidelines. The information presented in this report is based on a pilot study and, therefore, it is suggested that this information be viewed as a general guide until further research is carried out. The intent of this report is to suggest an economical connection detail and outline a procedure to comprehend its behavior through the behavioral model presented.

7.2 Scope for further studies

In this investigation, only one 1/2 scale model of the through beam connection was tested under monotonic loading. To standardize the design procedure for through connection detail more number of tests are recommended. Also, it would be interesting to (1) study the behavior of through connection detail under cyclic loading, (2) study the effect of

applying axial load on column, (3) study the effect of connecting beams to column in both directions.

REFERENCES

1) Ansourian,P., "Connections to concrete-filled tube columns", IABSE volume 36-I, April 1976.

2) Ansourian,P., "Composite connections to external columns", ASCE, ST 8, August 1976, pp 1609-1625.

3) Ansourian,P., "Shear in composite beam-column connections", Proc. Inst. Civil Engrs., Part 2, December 1981, pp 1131-1147.

4) "ANSYS Engineering Analysis System", Swanson Analysis Systems Inc., Houston, PA, October 1989.

5) Azizinamini,A., Prakash,B., Prishtina,B. and Salmon,D., "New steel beam to composite column connection", Composite construction II conference, Missouri, June 1992.

6) Azizinamini,A., Prakash,B., Prishtina,B. and Salmon,D., "Through connection detail for composite columns in high-rise buildings", Structural stability research council (SSRC) conference, Pittsburgh, April 1992.

7) Chaiki,M., Shosuke,M., Hiromichi,M. and Keigo,T., "New type of composite beam-to-column connection using embossed wide flange steel shape", Composite construction in steel and concrete, ASCE, June 1987.

8) Charles Raths, "Embedded structural steel connections", PCI journal, May-June 1974, pp 105-112

9) Chen,W., and Chen,C., "Analysis of concrete-filled steel tubular beam columns", Volume 33-II, IABSE, 1973, pp 37-52

10) Daniel,H., Kroll,G., and Fisher,J., "Behavior of composite beam to column joints", ASCE, ST3, March 1970, pp 671-685.

11) Dawe and Grondin, "W-shape beam to RHS column connections", Canadian journal of civil engineering, # 17, 1990, pp 788-797.

12) Dierlein,G., "Design of moment connections for framed structures", Doctoral dissertation submitted to University of Texas at Austin, May 1988.

13) Hal Iyengar, "Recent developments in mixed steel-concrete systems", Composite and Mixed construction, ASCE, July 1984.

14) Hawkins and Mitchel, "Moment resisting connections for mixed construction", AISC engineering journal, Ist quarter 1980, pp 1-10.

15) Hiroshi,K., Mototsugu,T., Teruyasu K., Ji,H., and Mikio,I., " A study of concrete filled RHS column to H-beam connections fabricated with HT bolts in rigid frames", Composite construction in steel and concrete, ASCE, June 1987, pp 614-635.

16) Le-Wu Lu and Ben kato, "Research on composite elements and structures", Composite construction in steel and concrete, ASCE, June 1987.

17) Mattock and Gaafar, "Strength of embedded steel sections as brackets", ACI journal, March-April 1982, pp-83-93.

18) Mitchel and Kostas, "Precast concrete connections with embedded steel members", PCI journal, July-August 1980.

19) Prestressed Concrete Institute (PCI), "PCI design handbook - precast and prestressed concrete", 3rd edition, 1985.

20) Shakir-Khalil, "Full scale tests on composite connections", Private correspondence, July 1992.

21) Shao-Huai, "Ultimate strength of concrete-filled tube columns", Composite construction in steel and concrete, ASCE, June 1987, pp 702-727.

22) Sheikh Taquir, "Moment connections between steel beams and concrete columns", Doctoral dissertation submitted to University of Texas at Austin, December 1987.

23) Sheikh,T., Deierlein,G., Yura,J., and Jirsa,J., "Beam-column moment connections for composite frames", Part I and II, ASCE Journal of structural engineering, November 1989, pp 2858-2896.

24) Shosuke Morino, Jun Kawaguchi, Chihiro Yasuzaki and Satoshi Kanazawa, "Elasto-plastic behavior of concrete filled steel tubular three dimensional subassemblages", Private correspondence, July 1992.

25) Tatsuo,O., Toshimoto,M., Toshiharu,H., Kiyoshi,K., and Hidekazu,N., "An experimental study on rectangular steel tube columns infilled with ultra-high strength concrete cast by centrifugal force", International symposium on Tubular structures, September 1989.

26) Virdi and Dowling, "Bond strength in concrete filled steel tubes", IABSE proceedings, 3/1980, pp 33-80.